Characterization and Application of Nanomaterials 2026, 9(1), 026060003.
https://doi.org/10.24294/can026060003

Review

Rice husk ash (RHA) in materials engineering: Four decades of processing, performance, and pathways to industrialization

Ashok Kumar Mishra[1]*, Thakur Abhinav Amar[2]

[1] Department of Mechanical Engineering, SRM University, Delhi-NCR, Haryana 131029, India
[2] Department of Production & Industrial Engineering, BIT Mesra, Ranchi, Jharkhand 835215, India
* **Corresponding author:** Ashok Kumar Mishra; akmishra@srmuniversity.ac.in

CITATION

Mishra A K, Amar T A. Rice Husk Ash (RHA) in Materials Engineering: Four Decades of Processing, Performance, and Pathways to Industrialization. Characterization and Application of Nanomaterials. 2026; 9(1): 026060003. https://doi.org/10.24294/can026060003

ARTICLE INFO

Received: 03 February 2026
Accepted: 13 May 2026
Available online: 22 May 2026

Abstract: This review provides a comprehensive, processing-centric synthesis of four decades (1986–2025) of rice husk ash (RHA) research, linking combustion chemistry, purification, mechanical activation, and fabrication routes to microstructural evolution and material performance in metal matrix composites (MMCs), cementitious systems, and geopolymers. A consistent finding is an optimal reinforcement window of 4–10 wt.% RHA, achieving significant improvements in hardness (32–55%), tensile strength (28–38%), wear resistance (40–60%), compressive strength (10–25%), elastic modulus (10–30%), and damping capacity (18–35%), while avoiding particle clustering and porosity at higher loadings. Fabrication routes including stir casting (scalable, 2–10 wt. % RHA), powder metallurgy/spark plasma sintering (superior densification, 0–20 wt. % RHA), and friction stir processing (40–50% surface hardness increase) are critically evaluated. Hybrid reinforcements—RHA-SiC (55–75% hardness), RHA-B_4C (40–60% wear resistance), RHA-CNT/graphene (25–40% fracture toughness), and RHA-graphite (10–25% friction reduction)—overcome monolithic RHA brittleness. In cementitious applications, 10–20% RHA replacement of Portland cement enhances long-term strength, reduces chloride penetration by 30–50%, and achieves 15–30% theoretical CO_2 reduction. Emerging AI/ML approaches (ANN, SVR, random forest, XGBoost-SHAP) achieve predictive accuracy of $R \approx 0.94$–0.99 for mechanical and tribological properties. Critical barriers to industrial deployment include lack of standardized RHA characterization, limited pilot-scale validation, and scarce life-cycle assessment data. A prioritized roadmap addresses standardization, interface engineering databases, pilot demonstrators, AI-ready data infrastructure, and alignment with circular economy principles and ASTM/ACI standards.

Keywords: rice husk ash; stir casting; spark plasma sintering; friction stir processing; geopolymer; sustainability; artificial intelligence

1. Introduction

1.1 Background and motivation

Rice husk ash (RHA) is generated from the combustion of rice husks, an agricultural by-product constituting roughly 20% of the rice grain mass. When burned under controlled conditions (500–700 °C), rice husk yields amorphous silica with high surface area and reactivity, making it a promising reinforcement or supplementary binder material [1–5].

Historically, disposal of rice husks and ash led to environmental challenges, including open-air burning, landfilling, and particulate emissions [5]. Early research in the late 1980s and 1990s concentrated on silica extraction and purification from RHA [3,4]. By the 2000s, the focus expanded to metal matrix composites (MMCs),

where RHA contributed to improved hardness, tensile strength, and wear resistance [6–12]. In the 2010s and 2020s, RHA gained prominence in cementitious and geopolymer systems due to its high pozzolanic activity, contributing to reduced CO_2 emissions and enhanced material durability [13–19].

Recent interest also includes hybrid composites (e.g., RHA + SiC, B_4C, CNTs), AI-based performance prediction, and sustainability-driven applications such as pervious concrete and recycled aluminum alloys [20–26]. The breadth of this evolution necessitates a comprehensive, chronologically structured review [27].

While numerous reviews have cataloged the properties of RHA in specific applications (e.g., concrete or aluminum composites), a critical synthesis is lacking. Existing works often treat RHA as a static filler, neglecting how its evolving processing science—from raw husk to engineered nanoparticle—dictates four decades of performance outcomes. Furthermore, there is no integrative analysis that connects historical research phases to current sustainability imperatives and data-driven material design. This review addresses that gap by providing a processing-centric narrative, tracing the evolution of RHA from silica extraction to multifunctional hybrids, and explicitly evaluating each fabrication route through the dual lenses of performance optimization and industrial scalability.

1.2. Composition and physical properties of rice husk ash

Rice husk contains approximately 15–20 wt.% silica, primarily concentrated in the outer epidermis. Controlled burning yields amorphous silica (SiO_2), whereas burning above 900–1000 °C produces crystalline forms (quartz, cristobalite) with reduced reactivity [6,21]. **Table 1** summarizes the key physical and chemical properties of RHA. Key physical and chemical characteristics of RHA that influence its performance as a reinforcement and supplementary cementitious material. The low density (1.8–2.2 g/cm³), high amorphous silica content (80–95%), and high surface area make RHA suitable for lightweight composites and pozzolanic applications.

Table 1. Physical and Chemical Properties of Rice Husk Ash.

Property	Typical Value / Description	Key Reference
Density	1.8–2.2 g/cm³	[28]
Amorphous silica content	80–95% (dependent on combustion control)	[29]
Minor oxides	K_2O, CaO, MgO	[30]
Surface area	High porosity and surface area	[31]
Particle morphology	Irregular, porous	[28]
Crystallization temperature	>900–1000 °C (quartz, cristobalite)	[12]

Mechanical and pozzolanic roles of RHA include enhancement of hardness and tensile strength in MMCs through load transfer and grain refinement mechanisms [8,11,12,32].

1.3. Evolution of research (1986–2025)

RHA research can be mapped into five chronological phases, corresponding to technological focus shifts. **Table 2** demonstrates the transition from fundamental silica extraction to advanced multifunctional materials and sustainable construction applications. Chronological evolution of RHA research across five distinct phases, from fundamental silica extraction to AI-driven optimization and sustainable construction. Each phase represents a paradigm shift in processing, applications, or performance targets.

Table 2. Phases of RHA research development (1986–2025).

Phase	Years	Key Research Themes	Representative Contributions
I	1986–2003	Silica extraction; early Al/RHA composites	Silica recovery; first MMC trials [3,4,6,7]
II	2008–2010	Geopolymer precursors; RHA degradation studies	Aluminosilicate formation; chemical activation [19,33]
III	2011–2015	Strengthening, wear behavior, hardness optimization	Taguchi/DOE studies; hybrid reinforcements [34–36]
IV	2016–2019	Hybrid composites: SiC, B_4C, TiC, MgO, rare-earths	Interface-engineered MMCs; high-performance hybrids [37–39]
V	2020–2025	Sustainability, AI/ML, recycled alloys, SCMs	Green concrete; ML-supported optimization [40–46]

1.4. Objectives of the review

This review aims to:

1. Provide a chronologically-structured, critical synthesis of global RHA research from 1986 to 2025, highlighting paradigm shifts.
2. Establish causal links between RHA processing parameters (combustion, purification, milling) and the resulting microstructure in composite and cementitious systems.
3. Consolidate and explain trends in mechanical, tribological, and functional properties, identifying universal optima and trade-offs.
4. Critically evaluate hybrid and functional composite strategies, assessing their viability for overcoming single-reinforcement limitations.
5. Synthesize findings on cementitious and geopolymer applications to quantify RHA's role in sustainable construction.
6. Integrate emerging AI/ML approaches as a transformative tool for predictive modeling and inverse design of RHA-based materials.
7. Propose a prioritized, actionable roadmap to overcome scientific, technical, and standardization barriers to industrial adoption.

2. Processing of rice husk ash

Effective use of rice husk ash depends strongly on the processing route. Parameters such as combustion temperature, duration, chemical treatment, mechanical activation, and post-processing techniques influence the resulting phase composition (amorphous vs. crystalline silica), particle size, porosity, and surface chemistry. These factors subsequently govern performance in composites, cementitious systems, and hybrid materials. RHA properties depend strongly on combustion conditions, pretreatment, and milling intensity [28,29,47]. **Figure 1** summarizes the standard processing flow from raw husk collection to final application pathways.

Figure 1. Processing Flow of RHA.

2.1. Controlled combustion and calcination

Controlled combustion is the primary step in converting rice husk into reactive silica-rich ash. The temperature window of 500–700 °C produces amorphous silica, which offers high reactivity and is favored for metal matrix composites, pozzolanic cementitious systems, geopolymers, and nano-silica precursors [4,21,23,48]. Temperatures exceeding 900–1000 °C cause silica to transition to crystalline phases (quartz, cristobalite), reducing reactivity and bonding efficiency in MMCs as well as pozzolanic activity [12,21].

Slow heating rates promote amorphous silica retention, whereas dwell times exceeding five hours increase crystallization tendency. Insufficient husk washing introduces alkali impurities that raise the melting point and cause glassy slag formation. Key early studies demonstrated that optimized combustion reduces carbon content and enhances silica purity, laying the foundation for RHA-based reinforcements and binders [3,6].

2.2. Chemical treatment and purification

Chemical treatment is typically used to enhance purity and surface activity and to remove alkali impurities that would otherwise interfere with composite bonding or pozzolanic reactivity [28,29].

Acid leaching using HCl, H_2SO_4, or HNO_3 removes metallic impurities (K, Ca, Mg), increases silica content above 95 wt.%, and improves reactivity and surface energy [31,49,50]. Well-controlled acid treatments produce highly reactive amorphous silica suitable for MMCs and geopolymer precursors [19,33].

Ionic liquid extraction is a modern method achieving ultra-high silica purity (≈99.6%) with enhanced surface area and controllable porosity. Alkaline extraction converts silica into sodium silicate solutions, useful for geopolymer precursor synthesis, binder systems, and sol-gel derived nano-silica powders [51].

2.3. Mechanical activation and nanostructuring

Mechanical milling controls particle size distribution and enhances microstructural uniformity [52]. Ball milling for 20–80 hours produces nano-RHA with average particle sizes below 100 nm [44,53]. Attrition milling refines particles for high-performance MMCs. Benefits include enhanced dispersion in molten metals, reduced clustering, increased reactivity for cementitious and geopolymer systems, and improved surface area. Nano-RHA has been shown to improve hardness, tensile strength, and wear resistance more effectively than micron-sized RHA, even at lower wt.% loadings [54].

2.4. Surface modification for improved wettability

Ceramic coatings such as Si_3N_4 reduce the Al/RHA contact angle from approximately 72° to 35°, improve infiltration of molten metal, and enhance interfacial bonding strength [55,56]. Rare-earth oxide treatments using Y_2O_3 or Pr_6O_{11} enable formation of beneficial interfacial layers, improved grain refinement, and higher hardness and wear resistance [18,57,58].

2.5. Functionalization for cementitious systems

RHA is widely used as a Supplementary Cementitious Material because it reacts with calcium hydroxide to produce additional C-S-H gel [40,41,59]. Critical processing requirements include fine grinding (below 45 μm) to improve packing density and reaction kinetics, de-carbonization to ensure no unburned carbon remains, and chemical activation (e.g., alkaline treatment) to accelerate pozzolanic reactions. Hybrid RHA-CNT and RHA-graphene systems with 0.1–0.2 wt.% nanocarbon additions improve microcrack bridging, shrinkage control, and tensile performance.

2.6. Summary of processing routes

Table 3 summarizes the major RHA processing routes and shows how combustion, chemical purification, and mechanical treatment influence silica phase, purity, particle size, and application suitability. It highlights the trade-offs between reactivity, cost, and processing complexity across different routes.

Table 3. Processing routes for RHA and their effects.

Processing Route	Key Features	Advantages	Limitations	Representative References
Controlled Combustion (500–700 °C)	Produces amorphous silica	High reactivity; best for MMCs & SCMs	Requires precise temperature control	[4,21,22]
High-Temp Calcination (>1000 °C)	Crystalline silica formation	High stability	Lower reactivity	[12,21]
Acid Leaching	Removes impurities	High-purity SiO_2 (>95%)	Handling corrosive agents	[19,33]
Ball Milling	Particle size reduction	Nano-RHA (<100 nm)	Time-consuming	[44,53]
Surface Coating (Si_3N_4)	Improves wettability	Contact angle reduction	Additional processing step	[55]

3. Fabrication routes for RHA-based composites

The efficacy of rice husk ash as a reinforcement material in composite systems is profoundly influenced by the selected fabrication route [1,4,8,60–64]. The processing methodology dictates critical microstructural characteristics—including reinforcement distribution, interfacial bonding integrity, and porosity—which in turn govern the final mechanical, thermal, and tribological properties. **Figure 2** summarizes the principal fabrication routes used for RHA-based composites, including stir casting, compocasting, powder metallurgy, spark plasma sintering (SPS), friction stir processing (FSP), infiltration techniques, and hybrid processing routes [4,62].

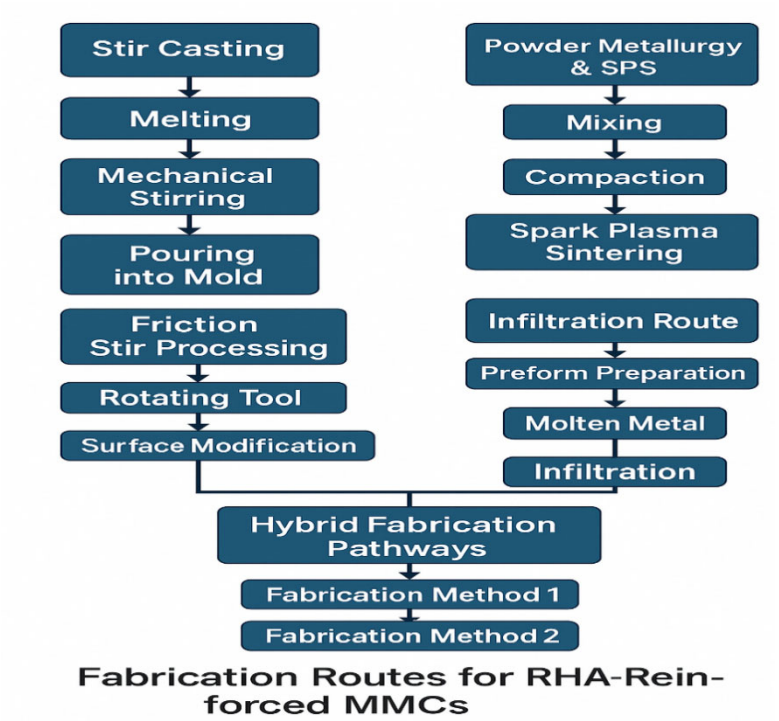

Figure 2. Fabrication Routes for RHA-Reinforced MMCs.

3.1. Powder preparation and pre-processing

The foundational step for virtually all fabrication methods is the pre-processing of raw RHA to ensure consistent quality and performance [28,47,50,65]. The inherent variability of as-produced RHA necessitates drying at 100–150 °C to eliminate adsorbed moisture, which can otherwise cause gas entrapment and porosity during liquid-state processing [28]. Sieving regulates particle size distribution and prevents inclusion of oversized particles that act as stress concentrators [30,66]. Mechanical grinding or milling reduces particle size, breaks down soft agglomerates, and increases specific surface area, thereby enhancing reactivity and potential for uniform dispersion within the matrix [31,50]. High-energy ball milling can produce nano-structured RHA, which significantly increases surface energy and pozzolanic reactivity, promoting stronger matrix bonding [44,53]. Acid leaching with HCl or H_2SO_4 dissolves metallic impurities and residual alkalies, yielding high-purity silica content often exceeding 95–99% [31,55]. This is particularly critical for applications requiring enhanced

thermal stability or chemical resistance. The overarching importance of these pre-processing steps is to minimize particle clustering, ensure homogeneous mixing with the matrix material, and improve the wetting behavior of RHA in molten metal systems.

3.2. Stir casting

Stir casting remains the most commercially prevalent and industrially scalable technique for fabricating RHA-reinforced aluminum matrix composites, prized for its cost-effectiveness and simplicity [4,37,58,61,62]. The method involves incorporation of RHA particles into a vortex created within a crucible of molten matrix alloy via mechanical stirring. The matrix alloy (commonly A356, AA6061, or AA7075) is superheated above its liquidus to maintain a slurry state during particle addition. RHA particles are preheated to 500–800 °C to remove surface moisture and gases and to reduce thermal shock upon introduction, which is important to prevent particle cracking and improve wetting. The preheated particles are introduced into the vortex at a controlled feed rate while maintaining a typical stirring speed of 400–800 rpm to ensure uniform distribution. The resultant mixture is poured into preheated molds and allowed to solidify.

Advantages include high cost-effectiveness, adaptability for mass production, and capability to produce complex and near-net-shaped components [67], with demonstrated efficacy for RHA weight fractions typically ranging from 2% to 10% [68,69]. Limitations include a tendency for particle agglomeration and segregation due to density differences and poor wettability, propensity for gas entrapment and oxide inclusion leading to porosity, and challenges in achieving uniform distribution especially with higher weight fractions or finer particles. Process enhancements such as ultrasonic assisted stir casting (which disrupts agglomerates and degasses the slurry), two-stage (double) stirring (improving distribution by stirring in both fully liquid and semi-solid states), and wetting agents like magnesium or rare earth elements (0.5–1 wt. %) improve wettability of ceramic RHA by molten aluminum [70].

3.3. Compocasting (semi-solid metal processing)

Compocasting is a specialized variant of stir casting conducted within the semi-solid (mushy zone) temperature range of the matrix alloy [71,72]. RHA particles are incorporated into a vigorously stirred slurry consisting of spherical solid grains suspended in the liquid phase. The high viscosity of the semi-solid slurry reduces particle settling and floating, leading to superior distribution. Benefits include markedly improved particle distribution and retention, reduced turbulence and gas entrapment resulting in lower porosity compared to conventional stir casting, and fine-grained microstructure often exhibiting enhanced mechanical properties. This method is frequently combined with post-processing techniques like cold rolling for further grain refinement [73] and is well-suited for manufacturing medium-strength AMC components where improved fatigue resistance and homogeneity are key requirements.

3.4. Powder metallurgy and spark plasma sintering

Powder metallurgy routes offer superior microstructural control and are ideal for fabricating high-performance RHA composites, especially with hybrid reinforcements [69]. In conventional powder metallurgy, metal powder and pre-processed RHA are uniformly mixed using a ball mill or blender, then cold-pressed under high uniaxial pressure to form a "green" compact, followed by sintering in a controlled atmosphere furnace below the matrix solidus (typically 500–650 °C for Al alloys) to promote diffusion bonding and densification. Advantages include excellent control over reinforcement distribution and volume fraction, near-net-shape capability with minimal material waste, and ability to fabricate composites with complex or hybrid reinforcement systems (e.g., RHA + SiC, B_4C). Limitations include relatively higher cost compared to stir casting, possible residual porosity limiting density and mechanical properties, and limited scalability for large or complex components.

Spark plasma sintering is an advanced consolidation technique that utilizes a pulsed direct current and uniaxial pressure to achieve rapid densification. The powder blend is loaded into a graphite die and subjected to simultaneous high pressure and high-intensity pulsed DC current, generating rapid Joule heating at particle interfaces and facilitating surface cleaning and material transport. Benefits include extremely high densification with minimal grain growth due to short processing times, formation of clean and strong particle-matrix interfaces often superior to conventional sintering, and capability to process nano-structured and metastable materials. SPS is the preferred method for producing high-integrity MMCs for demanding applications in aerospace, defense, and wear-resistant engineering components.

3.5. Friction stir processing

Friction stir processing is a robust solid-state technique derived from friction stir welding, used for fabricating surface composites [1,74–78]. A non-consumable rotating tool with a specially designed pin and shoulder is plunged into the workpiece. RHA particles are packed into pre-machined grooves or holes on the substrate surface. The traversing tool generates intense frictional heat and severe plastic deformation, stirring the RHA particles into the surface layer and producing a dynamically recrystallized, fine-grained microstructure. Advantages include significant grain refinement and homogenization of the surface layer, very low porosity and excellent particle-matrix bonding, and substantial surface property enhancements with reported hardness increases of 40–50% [79]. Limitations include reinforced zone limited to a shallow surface layer, significant tool wear when processing with hard ceramic particles, and multi-pass strategy often required for large surface areas.

3.6. Pressure and vacuum infiltration

This technique is particularly suited for manufacturing composites with high reinforcement content or functionally graded materials. A porous preform composed of RHA and other ceramic particles is first fabricated. Molten metal is then infiltrated into the preform either under vacuum (to prevent gas entrapment) or in a pressureless manner, often aided by capillary action or a reactive metal (e.g., Mg in Al) that improves wettability. Benefits include capability to achieve very high reinforcement

loadings (up to 50–60 vol.%) and fabrication of bilayer or graded structures such as a hard wear-resistant surface layer bonded to a tough ductile core [80]. This is ideal for applications like brake rotors, liners, and other high-wear components. Limitations include complex process requiring careful preform preparation and potential for undesirable interfacial reactions between molten metal and ceramic preform.

3.7. Thermal spray and surface deposition techniques

These methods are exclusively used for applying RHA-reinforced coatings onto substrate materials [35]. High-velocity oxy-fuel propulsion of powder (metal + RHA) at supersonic speeds results in dense, well-bonded coatings. Cold spray utilizes kinetic energy rather than thermal energy to deposit particles, minimizing oxidative and thermal degradation of the feedstock. These techniques are employed to deposit wear- and corrosion-resistant coatings on steel or alloy substrates, extending component service life [42,81].

3.8. Additive manufacturing

The incorporation of RHA into additive manufacturing processes represents an emerging research frontier. RHA-derived silica or nano-RHA can be integrated into metal or polymer feedstocks for processes like binder jetting or selective laser melting to create lightweight bio-derived MMCs or ceramic lattice structures. Significant hurdles remain, including non-uniform melting characteristics of biogenic ash, need for precise powder morphology and flowability for AM processes, and ensuring consistent reinforcement distribution within the printed part [41].

3.9. Hybrid fabrication strategies

To synergize the benefits of individual techniques and overcome their inherent limitations, hybrid fabrication strategies are increasingly adopted [55,82,83]. Notable examples include stir casting followed by friction stir processing to locally refine microstructure and enhance surface properties; conventional powder metallurgy blending with subsequent SPS consolidation to achieve near-theoretical density; compocasting combined with cold rolling for further refinement and densification; and infiltration with tailored heat treatment cycles to relieve residual stresses and enhance interfacial strength. These integrated approaches demonstrate that strategic combination of methods can yield composites balancing cost-effectiveness with high performance [5,84,85].

3.10. Comparative summary

The choice of fabrication route is a decisive economic and technical compromise. While stir casting offers scalability, its inherent porosity and clustering issues (evident in the 2–10 wt.% loading limit) cap performance. Powder metallurgy routes, particularly SPS, achieve superior properties but at a cost that may preclude high-volume applications. This dichotomy underscores a central challenge for industrialization: advancing process modifications (e.g., ultrasonic stir casting) to elevate low-cost routes while driving down the cost of high-performance methods like SPS for critical sectors. **Table 4** compares key fabrication routes. Comparative

assessment of eight fabrication routes for RHA-reinforced composites, highlighting operating principles, key benefits, limitations, and typical RHA loading ranges. Stir casting offers scalability (2–10 wt. %) but suffers from porosity and clustering, while SPS provides superior densification (0–20 wt. %) at higher cost.

Table 4. Comparative summary of fabrication routes.

Method	Principle	Key Benefits	Limitations	Typical RHA wt.%	References
Stir Casting	RHA stirred into molten metal	Scalable, low cost	Porosity, clustering	2–10%	[68,69]
Compocasting	RHA added in semi-solid stage	Good distribution	More complex	2–10%	[73]
Powder Metallurgy	Powder blending + sintering	Uniform distribution	Lower density	0–20%*	[86]
Spark Plasma Sintering	DC-pulsed sintering	Highest density	High cost	0–20%	[18]
Friction Stir Processing	Surface layer reinforcement	40–50% hardness increase	Surface only	2–12%	[79]
Infiltration	Molten metal infiltrates preform	Graded materials	Preform complexity	High volume fraction	[85]
Thermal Spray	RHA-based powders deposited	Surface protection	Adhesion issues	Powder blends	[42]
Additive Manufacturing	Layered manufacturing	Complex geometries	Powder behavior issues	Experimental	[41]

*Higher RHA loading ranges are generally achievable in powder metallurgy and SPS routes due to improved dispersion and densification compared with liquid-state processing methods.

Stir casting typically handles 2–10 wt. % RHA due to agglomeration limits, while SPS and PM allow up to 20 wt.% because of better dispersion and densification.

4. Mechanical properties of RHA-reinforced composites

The mechanical performance of composites reinforced with rice husk ash is governed by a complex interplay of factors including composition, particle size, weight fraction of reinforcement, fabrication methodology, and resultant microstructural characteristics. A consistent finding across the literature is that optimized RHA incorporation, typically within 4–10 wt.%, leads to significant enhancements in hardness, tensile strength, and elastic modulus, albeit often with a trade-off in ductility and toughness.

4.1. Hardness

The hardness of the matrix alloy is one of the most reliably improved properties with RHA addition. Enhancement is attributed to several concurrent mechanisms: intrinsic load-bearing capacity of hard silica particles, significant increase in dislocation density due to thermal expansion mismatch between matrix and reinforcement, and grain refinement effect where RHA particles pin grain boundaries and inhibit grain growth [37,61,87–89]. Peak hardness is typically achieved at 6–10 wt.% RHA, beyond which agglomeration leads to property degradation [60]. Powder metallurgy routes, particularly SPS, consistently yield the highest hardness values due to superior densification, minimal porosity, and refined microstructure [18,86]. Friction stir processing is exceptionally effective for surface hardening, with documented microhardness increases of 40–50% in AA6xxx and AA7xxx series aluminum alloys [79]. **Table 5** presents representative hardness improvements. RHA

addition up to 6–10 wt. % significantly improves hardness; beyond this range, agglomeration leads to property degradation.

Table 5. Representative hardness improvements with RHA.

Alloy System	Fabrication Route	RHA (wt.%)	Hardness Increase (%)	Key References
AA6061	Stir casting	6%	32%	[68]
A356	Compocasting + Rolling	8%	41%	[73]
AA7075	FSP	10%	48%	[79]
Al-Mg alloy	PM / SPS	4%	55%	[18]

4.2. Tensile strength

The ultimate tensile strength and yield strength of RHA composites typically exhibit a peak at intermediate reinforcement levels. Strengthening is primarily governed by effective stress transfer from the ductile matrix to high-modulus RHA particles, Orowan looping around finely dispersed particles, and Hall-Petch strengthening from grain refinement [74,90–92]. The optimal tensile strength is generally achieved at 4–8 wt.% RHA [11,86]. Within this range, reinforcing benefits outweigh detrimental effects of incipient defects. Beyond 10–12 wt.%, tensile strength frequently declines due to particle clustering acting as stress concentration sites, increased porosity from inadequate wetting, and formation of weak interfacial zones. Stir-cast AA6061/RHA composites demonstrated 28–38% increase in UTS at 6–8 wt.% RHA loading [69].

4.3. Compressive strength

Compressive strength often shows more improvement with increasing RHA content compared to tensile strength [79]. Compressive loading modes suppress propagation of micro-cracks and reduce detrimental effects of particle-matrix decohesion and particle pull-out, which are dominant failure mechanisms under tension [44,53,93,94]. Improvements in compressive strength of 10–25% have been reported for both stir-cast and PM-processed composites [12,84]. Hybrid reinforcement systems such as RHA combined with SiC or B_4C have demonstrated synergistic effects leading to compressive strength improvements up to 40% [85].

4.4. Modulus of elasticity

The elastic modulus of a composite is a rule-of-mixtures dominated property. Since the modulus of silica is significantly higher than that of aluminum alloys, composite stiffness increases progressively with RHA fraction [44,93–95]. A 10–30% improvement in Young's modulus has been documented at RHA loadings of 4–10 wt.% [69,73]. Processes like PM and SPS, which ensure excellent interfacial bonding and high density, typically yield higher modulus values than stir-cast counterparts.

4.5. Impact energy and toughness

Incorporation of a brittle ceramic phase like RHA invariably influences fracture toughness and impact energy. A slight decrease in toughness with increasing RHA content is a common observation [10,35,39,85,96]. Stiff RHA particles increase overall brittleness and impede plastic deformation and ductile tearing, which are primary energy-absorption mechanisms in metals. Under impact loading, interfaces can become sites for crack initiation and propagation. To counter this embrittlement, hybrid reinforcement strategies with secondary ductile or lubricating phases such as graphite, carbon nanotubes, or graphene nanoplatelets have shown promise in partially recovering lost toughness without sacrificing excessive strength [45].

4.6. Strengthening mechanisms

The enhancement of mechanical properties in RHA-reinforced composites can be rationalized through several established strengthening mechanisms. Load transfer is fundamental—applied stress is effectively transferred from the softer metal matrix to high-modulus RHA particles via strong interfaces [82]. Orowan strengthening predominates with nano- and sub-micron RHA particles, where fine particles act as impenetrable obstacles forcing dislocations to bow and loop around them [24]. Thermal mismatch strengthening from significant difference in coefficient of thermal expansion between aluminum matrix and silica RHA generates high density of geometrically necessary dislocations in the matrix during cooling [97,98]. Grain refinement occurs as RHA particles pin grain boundaries during solidification or recrystallization, contributing to strength via Hall-Petch relationship [74,99]. Interfacial strengthening through particle surface treatments (e.g., Si_3N_4 coating) or matrix alloying elements (Mg, rare-earths) improves wettability and forms stable interfacial compounds [23,44,100].

4.7. Contradictions and limitations in mechanical performance

Although most studies report monotonic property improvements up to 10 wt.% RHA, some researchers observed reduced toughness beyond 6 wt.% due to particle clustering. Similarly, while amorphous silica is universally preferred for maximum reactivity, a few studies noted acceptable performance with crystalline silica under specific low-reactivity conditions where thermal stability is prioritized over pozzolanic activity. These discrepancies highlight the need for standardized RHA characterization protocols and application-specific optimization rather than universal optimum claims [101].

Figure 3 illustrates the variation of (a) Hardness increases up to 6–10 wt.% RHA due to grain refinement and dislocation pinning from hard silica particles, then declines due to agglomeration-induced porosity. (b) Tensile strength peaks at 4–8 wt.% RHA where load transfer efficiency is maximized before particle clustering creates stress concentrations. (c) Impact energy gradually decreases as brittle silica particles reduce ductility and energy absorption capacity. (d) Comparative bar chart shows SPS and FSP yield highest hardness and strength due to near-full densification, refined microstructure, and strong interfacial bonding [4,10,15,37–39,74,77,80,84,85,87,92,93,102].

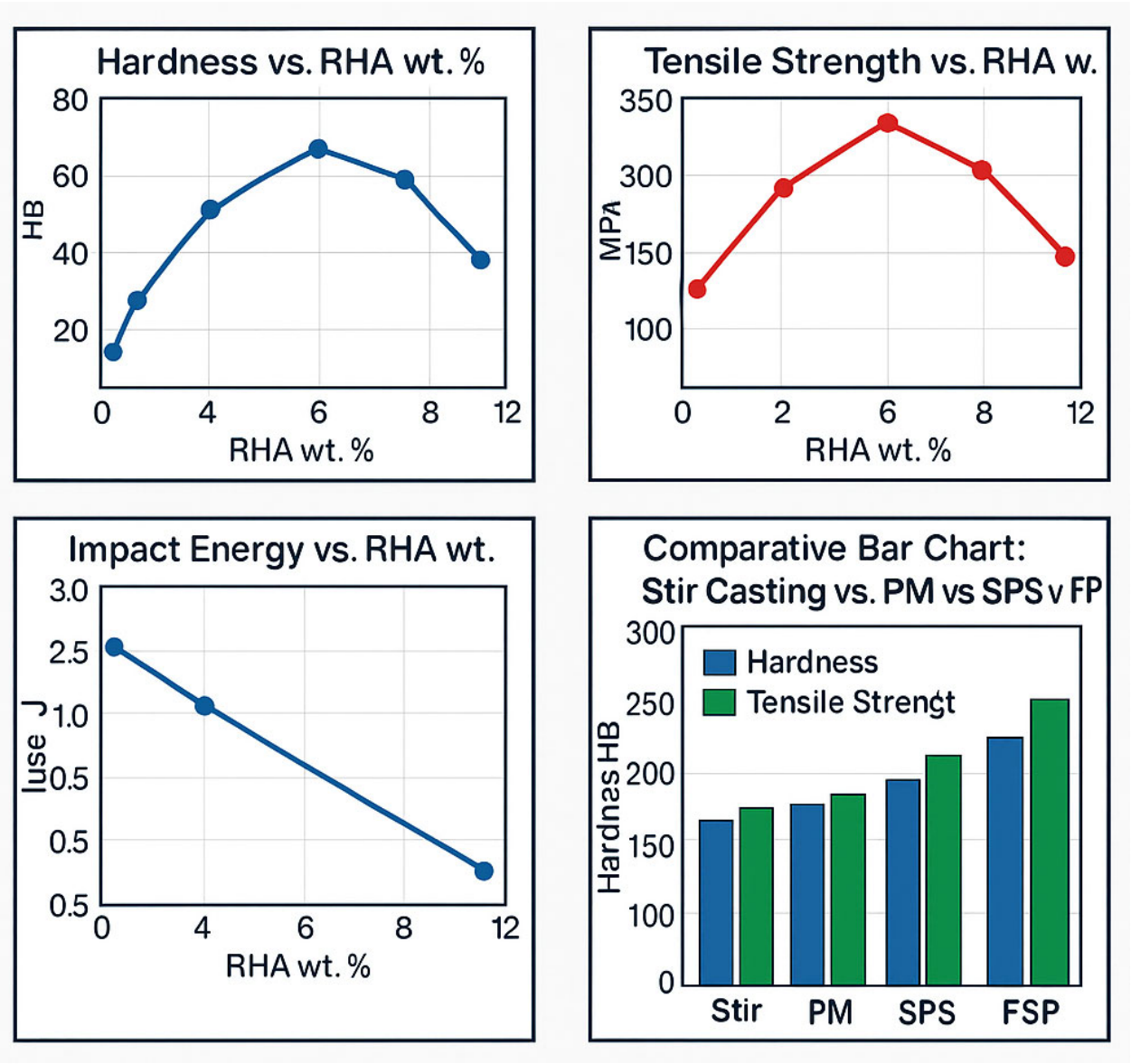

Figure 3. Mechanical Performance of RHA-Reinforced Composites.

5. Tribology and wear behavior

The tribological performance of RHA-reinforced MMCs is driven by intrinsic hardness and thermal stability of amorphous silica. Wear resistance is governed by RHA weight fraction, particle size, hybrid reinforcements, applied load, sliding velocity, and fabrication technique. A consistent finding is significant improvement in wear resistance up to an optimal RHA loading of 6–10 wt.%, beyond which benefits diminish due to particle clustering and increased porosity [85,88].

5.1. General wear behavior

Incorporation of RHA consistently reduces wear rate of aluminum alloys. This enhancement is attributed to load-bearing capacity of hard silica particles, grain refinement hindering dislocation motion and plastic deformation, and formation of stable tribo-oxidative films at elevated interfacial temperatures [53,79,85]. Hard silica particles contribute to wear resistance by acting as physical barriers against abrasive

counterfaces and by supporting applied loads, thereby protecting the softer metal matrix. The wear rate typically decreases with RHA addition up to approximately 10 wt.%, after which it can increase due to agglomeration-induced defects and porosity [68,69,103,104].

5.2. Effect of load and sliding velocity

Under low load and velocity conditions, the regime is characterized by mild abrasive and limited adhesive wear. RHA particles polish the surface, resulting in formation of stable oxide films and low wear rates [35,95]. Under high load and velocity conditions, the mechanism transitions to severe abrasive wear, oxidative wear, and delamination. Frictional heating softens the metal matrix, but RHA reinforcements help retain surface integrity. Hybrid systems (e.g., RHA-SiC) demonstrate superior stability under severe conditions [79,85,89,105].

5.3 Influence of RHA particle size

Particle size critically influences interfacial behavior and wear mechanisms. Nano-RHA (below 100 nm) offers highest surface area, leading to excellent dispersion and formation of compact protective tribo-layers, which significantly reduce wear rates [31,66,106]. Micron-sized RHA (above 20 μm) exhibits lower reactivity and relies on mechanical interlocking, with increased tendency for particle pull-out that can accelerate wear [3,8,68].

5.4. Predominant wear mechanisms

Abrasive wear dominates at low loads, characterized by micro grooving of the softer matrix by hard RHA particles [53,107]. Adhesive wear occurs through metal-to-metal contact and is mitigated by RHA particles acting as physical barriers between sliding surfaces [58,82,108]. Oxidative wear prevails at high sliding velocities, involving formation of lubricating oxide layers (glazes) that reduce wear rate [23,55,93]. SEM evidence consistently shows wear tracks with reduced delamination, fewer micro-cracks, and smoother morphology in RHA composites compared to unreinforced alloys.

5.5. Synergistic effects of hybrid reinforcements

Hybrid systems leverage strengths of multiple reinforcements for superior tribological performance. RHA + SiC/B_4C enhances hardness and high-temperature stability, leading to more stable tribolayer and reduced plastic deformation [99,107]. RHA + graphite reduces coefficient of friction by 10–25% through solid lubricant effect [39,85,96]. RHA + CNT provides crack-bridging elements, reducing delamination and improving toughness [78,108]. These combinations effectively mitigate limitations of monolithic RHA reinforcement such as brittleness while capitalizing on its hardness.

Figure 4 presents the variation of wear rate decreases up to 6–10 wt.% RHA (sweet spot) where hard silica particles stabilize sliding interface and form protective tribo-layers. Coefficient of friction declines more steeply with hybrid reinforcements (RHA-graphite, RHA-CNT) due to solid lubrication. Wear mechanism transitions

from mild abrasion (low load) to adhesive (medium load) to oxidative wear (high speed) where frictional heat promotes protective oxide glaze. Comparative bar chart shows SPS and FSP yield the highest wear resistance due to densification and microstructural refinement [15,22,23,38,39,53,61,74,82,88–90,96].

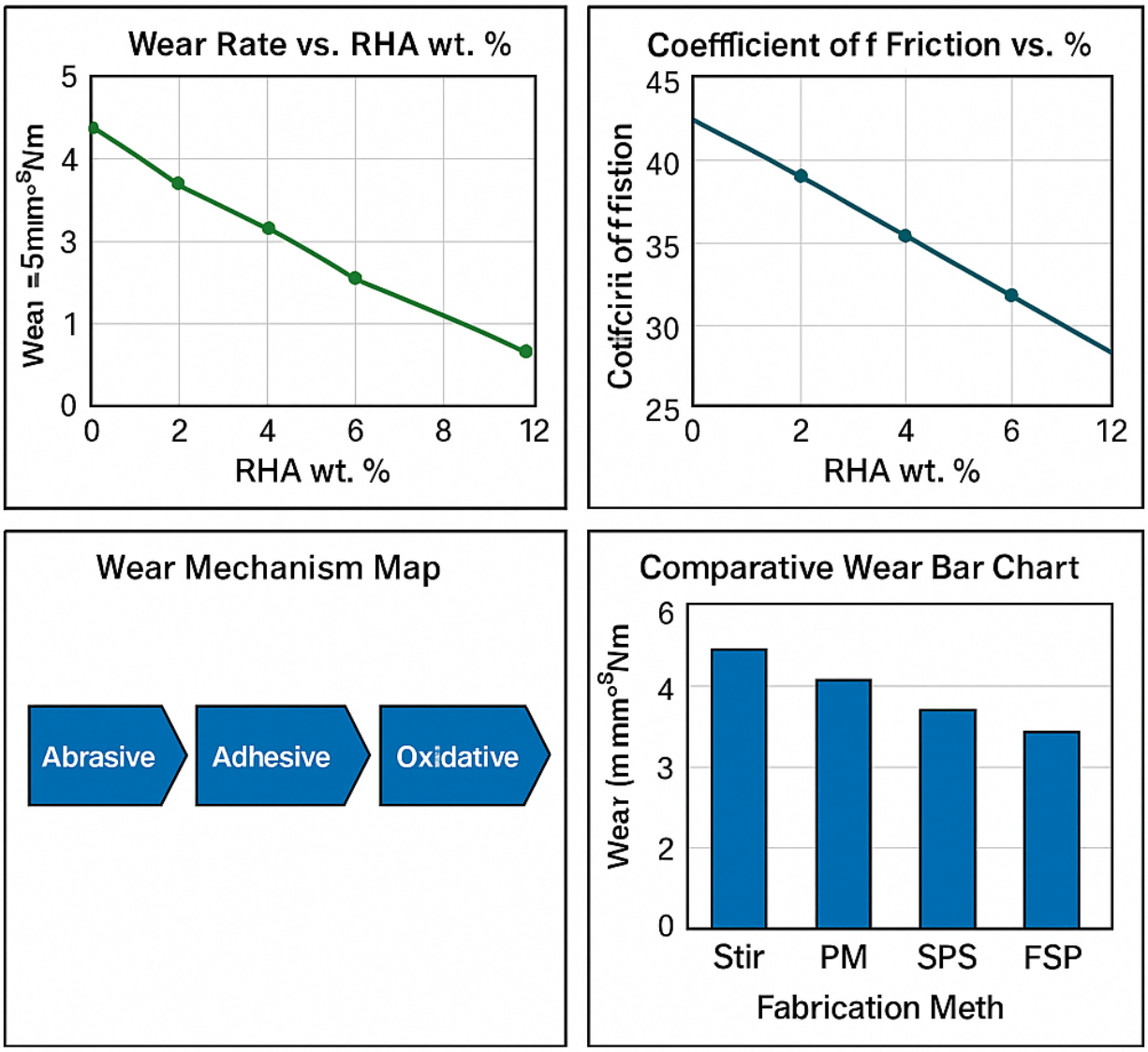

Figure 4. Tribology diagrams.

6. Functional properties of RHA-reinforced composites

Beyond mechanical and tribological performance, functional properties including corrosion resistance, thermal stability, damping capacity, and electrical conductivity are critical for automotive, aerospace, and marine applications [10].

6.1. Corrosion behavior

Corrosion resistance of RHA-reinforced AMCs is highly dependent on microstructural integrity [9,109]. Enhancement under optimal conditions occurs due to barrier protection where silica particles physically impede corrosive agent diffusion [6], passive film stabilization where RHA promotes more stable protective oxide

layers [10], and microstructural refinement reducing grain boundary area and limiting preferential corrosion pathways. Studies confirm improved corrosion resistance in NaCl and other environments for well-dispersed, high-purity RHA composites [53,110]. Conversely, corrosion resistance can be degraded by poor interfacial bonding creating crevice sites for pitting initiation, high porosity providing continuous pathways for electrolyte penetration, and particle clustering especially at high loadings (>12 wt.%) leading to localized galvanic corrosion [68,69,111,112].

6.2. Thermal properties

RHA significantly alters the thermal response of AMCs. Thermal conductivity reduction of 8–25% with 4–10 wt.% RHA occurs due to the intrinsically low thermal conductivity of silica, making composites suitable for engine covers and thermal insulators [38,39,88]. Thermal expansion (CTE) decreases as low-CTE RHA constrains matrix expansion, enhancing dimensional stability under thermal cycling [89].

6.3. Damping capacity

Incorporation of RHA enhances vibrational energy dissipation. The primary mechanism is increased interfacial friction at numerous RHA-matrix boundaries. Damping capacity improvements of 18–35% are reported for 6–10 wt.% RHA, with hybrid systems (e.g., RHA-graphite) showing further gains [113,114]. This property is valuable for reducing noise and vibration in structural components.

6.4. Density

With density of approximately 1.8–2.2 g/cm³, RHA is a lighter reinforcement compared to conventional ceramics like SiC (≈3.2 g/cm³). This enables 4–12% weight reduction in composites, offering significant advantages for lightweighting in transportation industries [89].

6.5. Electrical conductivity

As an electrical insulator, RHA reduces conductivity of the metallic matrix [115]. Additions of 4–10 wt.% RHA typically lead to 5–20% decrease in electrical conductivity. This property can be tailored for applications requiring specific electrical insulation or controlled EMI shielding, though hybridization with conductive phases like CNTs can partially mitigate loss.

Figure 5 illustrates the influence of corrosion rate decreases within 4–8 wt.% RHA where amorphous silica fortifies matrix and stabilizes passive films. Thermal conductivity declines with RHA addition due to intrinsically low conductivity of biogenic silica. Thermal expansion (CTE) decreases as rigid silica inclusions restrict lattice dilation. Damping factor increases with RHA addition, with hybrid composites (especially carbon-containing) absorbing 30–35% more vibrational energy [10,66,88,96,109,116].

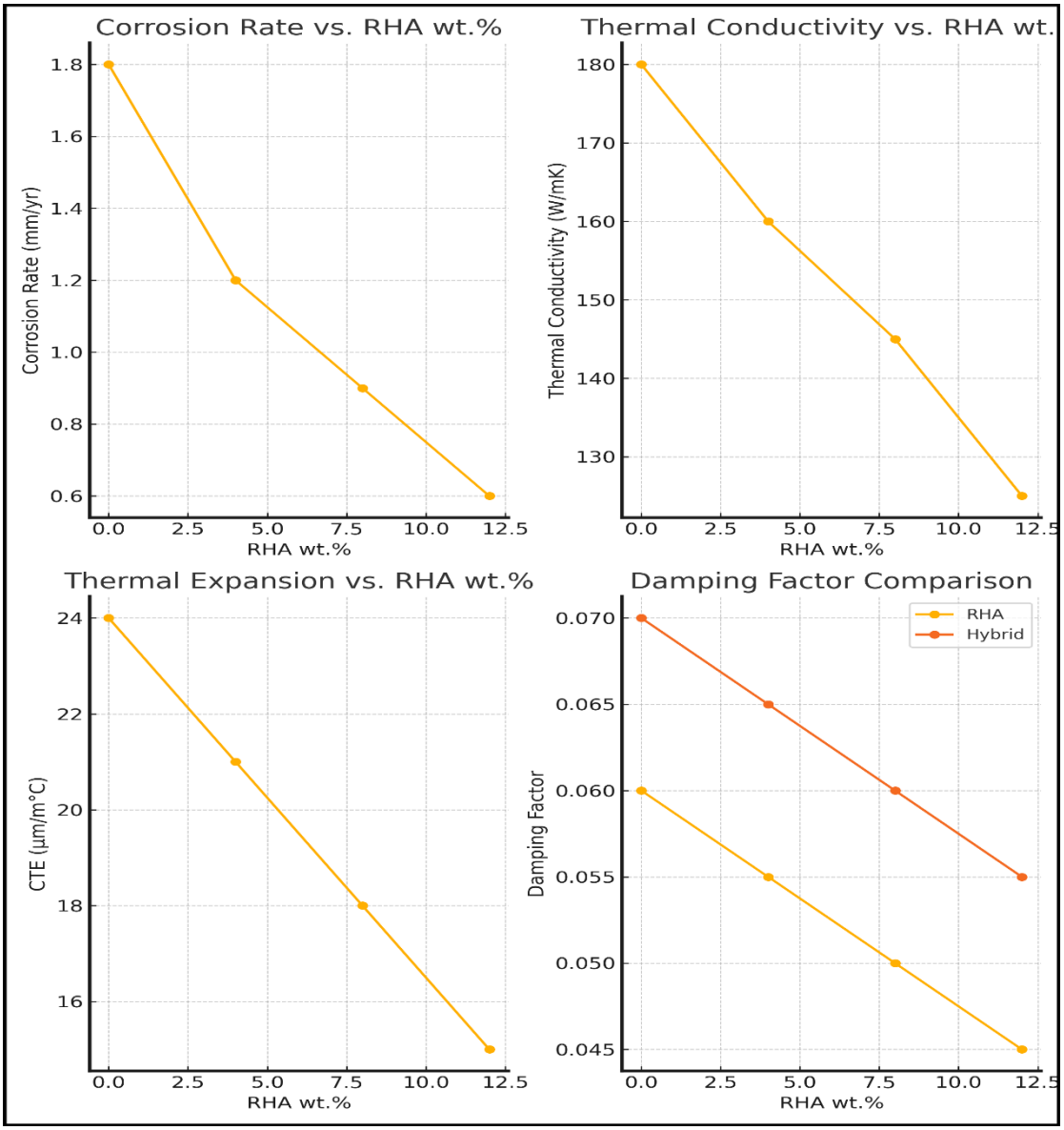

Figure 5. Functional properties.

6.6. Summary of functional properties

Table 6 summarizes functional property trends of RHA-reinforced composites, showing improved corrosion resistance, damping capacity, and thermal stability alongside reduced density and electrical conductivity. These property modifications enable lightweight design and multifunctional application. Summary of functional property modifications induced by RHA reinforcement, including corrosion resistance, thermal conductivity, thermal expansion, damping capacity, density, and electrical conductivity. RHA improves corrosion resistance (4–10 wt.%), damping capacity (18–35%), and reduces density (4–12%) but decreases thermal and electrical conductivity. These property modifications enable lightweight design and multifunctional application.

Table 6. Functional property trends of RHA-reinforced composites.

Property	Effect of RHA	Optimal Range	Governing Mechanisms	Key References
Corrosion Rate	Decreasing	4–10 wt.%	Passive film stabilization; barrier effect	[37,53,66]
Thermal Conductivity	Decreasing	4–10 wt.%	Intrinsic low conductivity of silica	[38,88]
Thermal Expansion (CTE)	Decreasing	4–12 wt.%	Constrained by stiff, low-CTE reinforcement	[89]
Damping Capacity	Increasing	6–10 wt.%	Energy dissipation at particle-matrix interfaces	[114]
Electrical Conductivity	Decreasing	All loadings	Insulating nature of silica phase	[69,115]
Density	Decreasing	2–12 wt.%	Low density of RHA reinforcement	[12,68]

7. Hybrid composites and functional materials

To overcome limitations of monolithic RHA reinforcement, such as inherent brittleness and limited interfacial strength, research has advanced into hybrid composites. By synergistically combining RHA with secondary reinforcements like SiC, B_4C, or carbon allotropes, it is possible to engineer materials with superior and multifunctional performance [20,63,78]. The pursuit of hybrid RHA composites, while promising, often lacks a systematic design framework. Many studies empirically combine RHA with SiC or CNTs without a priori modeling of synergistic or antagonistic interactions. For instance, simultaneous addition of brittle SiC and RHA may exacerbate fracture sensitivity unless a ductile phase (e.g., graphite) is incorporated. Future work must transition from trial-and-error to design principles based on complementary functionalities: using RHA for hardness and cost, CNTs for toughness and conductivity, and lubricants like graphite for tribological harmony [117].

7.1. RHA-SiC hybrid composites

This combination merges cost-effectiveness and low density of RHA with high hardness and stiffness of SiC. Hybrid systems demonstrate 55–75% improvement in hardness and significantly enhanced wear resistance compared to unreinforced alloys, attributed to synergistic grain refinement and formation of stable tribo-oxidative films [35,86,118,119]. Powder metallurgy and SPS routes yield the most pronounced microstructural benefits [15,69].

7.2. RHA-B_4C hybrid composites

B_4C complements RHA by providing exceptional hardness and high-temperature stability. These hybrids exhibit superior abrasion resistance and dimensional stability under thermal loads. Wear resistance improvements of 40–60% have been documented, making them suitable for severe sliding and heavy-load applications [22–24,107,120].

7.3. RHA-CNT and RHA-graphene hybrids

Addition of carbon allotropes introduces toughening and lubricating mechanisms. CNTs and graphene enable crack bridging and deflection, increasing fracture toughness by 25–40%. Their solid lubricant effect also reduces coefficient of friction

[78,92,102]. These hybrids partially restore electrical conductivity typically diminished by insulating RHA phase.

7.4. RHA-graphite hybrid composites

Graphite acts as solid lubricant within the composite [10,12]. This system shows substantial reduction in coefficient of friction and enhanced damping capacity, ideal for tribological components like bearings, bushings, and brake linings [51,68].

7.5. Rare-earth modified RHA composites

Addition of rare-earth oxides (Y_2O_3, CeO_2) serves as interfacial engineering strategy [18,57]. These elements enhance particle-matrix wettability, reduce porosity, and promote grain refinement, leading to improved fatigue resistance and bond strength.

7.6. Functionally graded materials

RHA is effectively used to create FGMs with a property gradient across the section. A hard wear-resistant surface layer (high RHA content) is integrated with a tough ductile core (low RHA content). This design benefits components like brake drums, rollers, and impact-resistant structures, minimizing residual stresses [5,121,122].

7.7 RHA-based coatings

RHA is incorporated into surface coatings via thermal spray (e.g., HVOF) and cold spray techniques, providing enhanced wear and corrosion protection as a low-density alternative to conventional ceramic coatings [55].

7.8. Additive manufacturing with RHA

Use of RHA in additive manufacturing is an emerging field [26]. RHA-derived silica is explored for metal and ceramic AM to create lightweight bio-derived structures. Key hurdles include controlling powder morphology and mitigating non-uniform melting behavior [41].

Figure 6 illustrates the interaction between RHA and various secondary reinforcements, Hybrid composite map shows RHA synergizing with SiC, B_4C, CNT, and graphite for enhanced hardness, wear resistance, lubrication, and toughness. An interface-engineering diagram illustrates coatings and rare-earth additives forming protective interfacial layers that improve wettability, reduce porosity, and stabilize grain boundaries. FGM structure shows hard wear-resistant surface transitioning to ductile core. Microstructure comparison contrasts uniform dispersion vs. graded architecture [3,5,18,24,35,37–39,53,68,70,78,80,85,118,122].

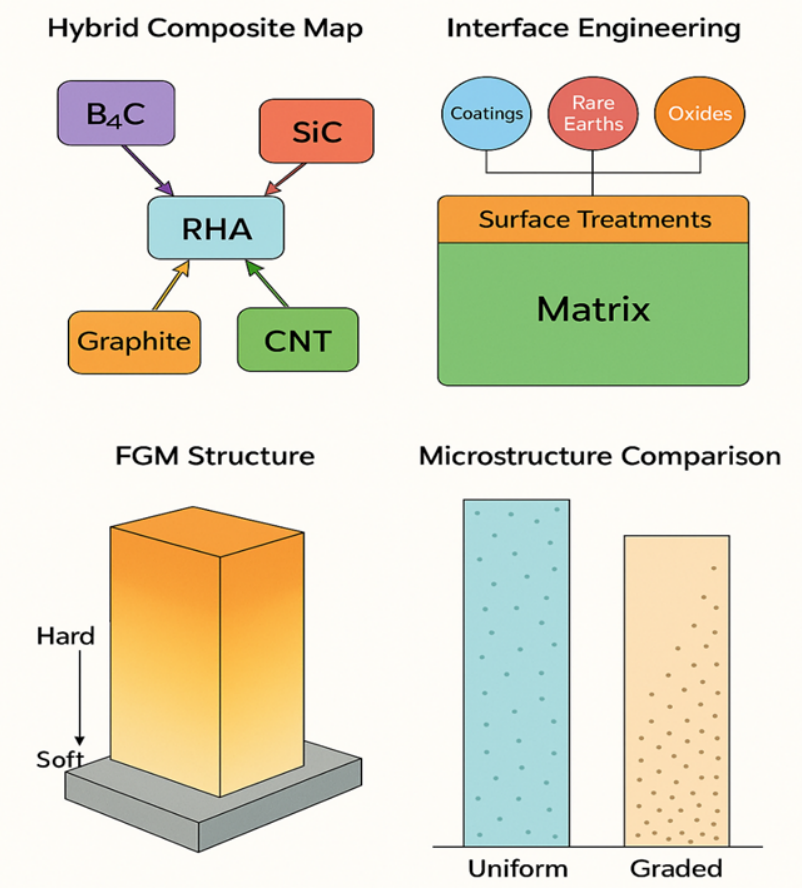

Figure 6. Hybrid composite map, interface engineering diagram, FGM structure, microstructure comparison.

7.9. Summary of hybrid systems

Table 7 present the performance summary of hybrid RHA composites combining RHA with secondary reinforcements (SiC, B_4C, CNT/graphene, graphite, rare-earth oxides). Each hybrid system offers distinct advantages: RHA-SiC (55–75% hardness increase), RHA-B_4C (40–60% wear resistance), RHA-CNT (25–40% fracture toughness), and RHA-graphite (10–25% friction reduction). Hybridization effectively overcomes the intrinsic brittleness of monolithic RHA composites by leveraging complementary reinforcement mechanisms, enabling tailored performance for demanding applications.

Table 7. Summary of hybrid RHA composite systems.

Hybrid System	Key Advantage	Primary Challenges	Typical Applications	References
RHA-SiC	55–75% hardness improvement	Fracture sensitivity	Wear-resistant parts	[35,86]
RHA-B_4C	40–60% wear resistance	High processing cost	Heavy-load components	[22,23]
RHA-CNT/Graphene	25–40% fracture toughness	CNT dispersion	Multifunctional composites	[78,102]
RHA-Graphite	10–25% friction reduction	Reduced strength	Bearings, bushings	[80,96]
Rare-earth + RHA	Improved wettability, grain refinement	High cost of rare-earths	High-performance MMCs	[18,57]

8. Cementitious and geopolymer applications

Rice husk ash, with its high amorphous silica content, is a widely utilized Supplementary Cementitious Material and key precursor in geopolymer synthesis. Its application enhances mechanical and durability properties of cementitious systems while significantly reducing carbon footprint associated with conventional construction materials [13,14,40,123].

8.1. RHA as a supplementary cementitious material

Partial replacement of Portland cement (typically 10–30% by weight) with RHA leads to enhanced long-term compressive strength, reduced permeability and improved durability, higher resistance to chemical attacks (sulfate, chloride), and significant reduction in embodied CO_2.

8.1.1. Pozzolanic reaction and workability

In this review, "pozzolanic activity" refers specifically to the reaction of amorphous silica with calcium hydroxide to form C-S-H gel in cementitious systems, distinct from its role in geopolymerization discussed in Section 8.3. The amorphous silica in RHA reacts with portlandite ($Ca(OH)_2$) to form additional calcium-silicate-hydrate gel, densifying the microstructure [13,45]. However, high surface area and irregular morphology of RHA particles can reduce workability, necessitating superplasticizers [20,45].

8.1.2. Strength development

While high RHA replacement levels may slow early-age strength gain due to dilution effect, continued pozzolanic reaction significantly enhances 28-day and long-term strength, with optimal performance at 10–20% replacement [14,45].

8.2. Microstructural and durability enhancements

Incorporation of RHA refines pore structure, reducing capillary porosity and pore connectivity as evidenced by SEM and MIP studies [45,46]. This densification, coupled with consumption of $Ca(OH)_2$, leads to improved sulfate resistance by reducing vulnerable portlandite content, reduced chloride penetration crucial for marine and de-iced structures [14], and control of alkali-silica reaction where high silica content helps sequester alkalis, mitigating expansive ASR [20].

8.3. High-performance and geopolymer concretes

RHA is effectively used in high-performance concrete and self-compacting concrete to enhance durability and adjust rheology [42,79]. In geopolymers, RHA serves as a silica source, reacting with alkaline activator and other aluminosilicates (e.g., fly ash, slag) to form N-A-S-H or C-A-S-H gels, resulting in binders with high early strength, excellent thermal resistance, and substantially lower CO_2 emissions compared to ordinary Portland cement [20].

8.4. Sustainability and life-cycle considerations

Hybridization of RHA with other materials, such as carbon nanotubes for crack control or metakaolin/slag for synergistic reactivity, further enhances performance

[45,46,89]. The primary sustainability benefit stems from utilizing agricultural waste to displace cement, whose production is a major global CO_2 source. Replacing 10–20% of cement with RHA can achieve 15–30% theoretical reduction in associated CO_2 emissions, promoting the circular economy [14] However, reproducible LCA data remain limited; most CO_2 reduction claims are based on cement displacement rather than full supply chain analysis, including transportation, grinding, and pretreatment. Future work should include third-party verified LCAs to substantiate sustainability claims.

Figure 7 illustrates the influence of RHA on compressive strength, durability, pore refinement, and geopolymer gel formation in cementitious systems. The figure demonstrates that moderate RHA incorporation enhances calcium silicate hydrate (C–S–H) gel formation and reduces pore connectivity, thereby improving long-term strength and durability [41]. Hybrid geopolymer systems containing fly ash or slag exhibit superior microstructural stability and reduced permeability. Adapted and modified from previous cementitious and geopolymer studies [19,59].

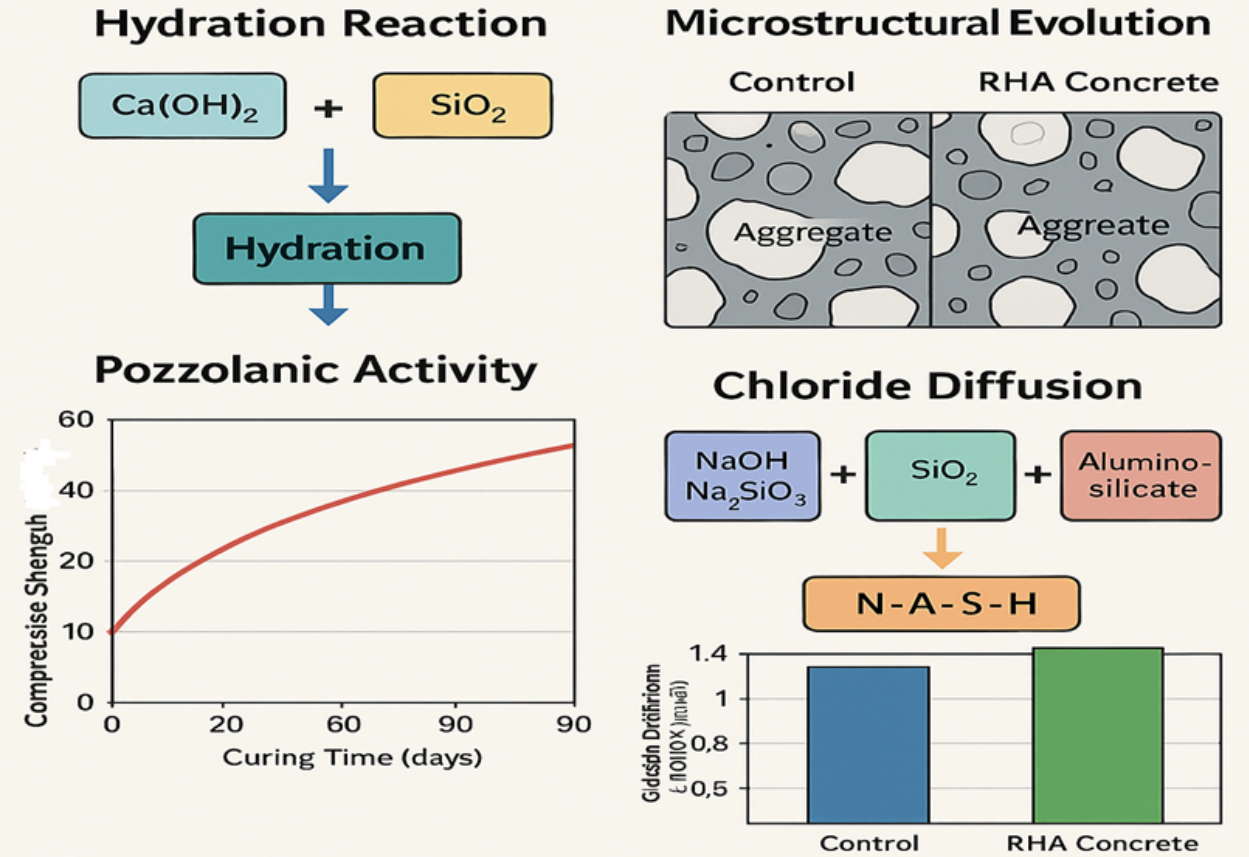

Figure 7. Microstructural and chemical evolution in RHA-modified cementitious systems.

Figure 8 illustrates the dual role of RHA in geopolymer binders and metal matrix composites. The Geopolymer Reaction Schematic shows RHA as a primary silica source reacting with alkaline activators ($NaOH/Na_2SiO_3$) and aluminosilicates (fly ash, slag) to form N-A-S-H or C-A-S-H gels, producing a cement-free binder with high early strength and thermal resistance. The Hybrid Composite Map and Interface Engineering Diagram demonstrate how RHA synergizes with secondary reinforcements (SiC, B_4C, CNTs, graphite) and surface coatings (Si_3N_4, rare-earth

oxides) to enhance hardness, wear resistance, and fracture toughness. The Functionally Graded Material (FGM) diagram depicts a graded architecture with a hard RHA-rich surface transitioning to a tough ductile core, enabling components to withstand abrasion while maintaining impact resistance. Collectively, **Figure 8** reinforces that RHA is not merely a filler but an active, engineerable component in both sustainable construction and high-performance composites.

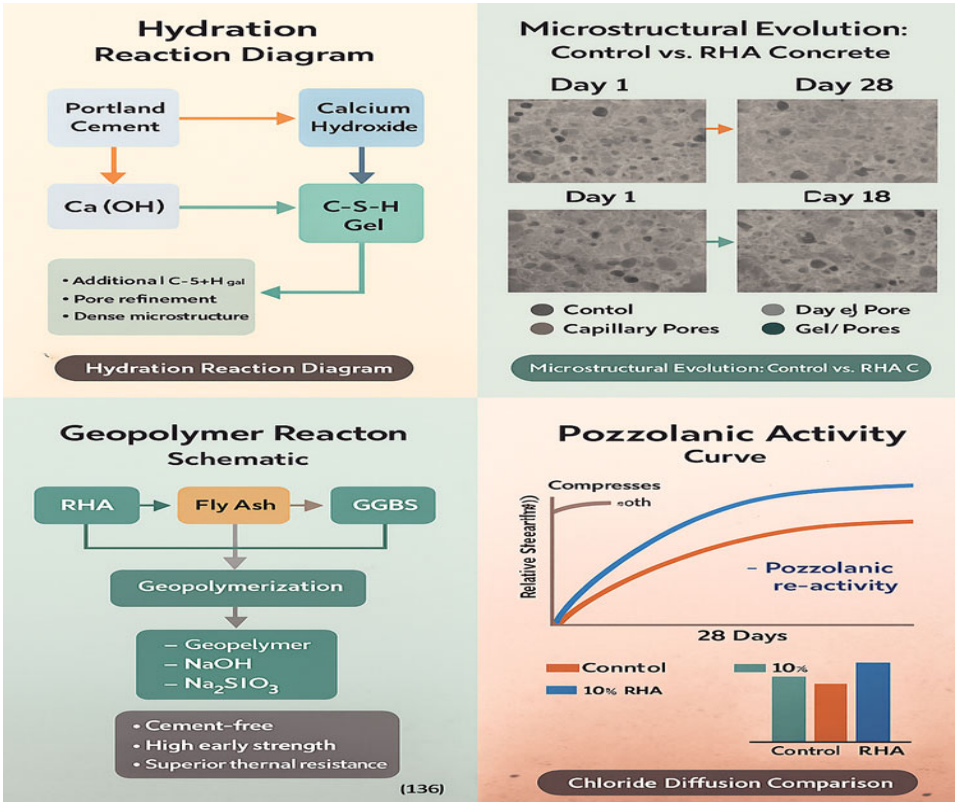

Figure 8. RHA in Geopolymerization and Composite Material Design.

Table 8 summarizes RHA performance as a supplementary cementitious material and geopolymer precursor. Optimal replacement levels (10–20%) enhance compressive strength, reduce chloride penetration (30–50%), improve sulfate resistance, and mitigate alkali-silica reaction. Geopolymer binders achieve high early strength with significantly lower CO_2 emissions.

Table 8. Cementitious and geopolymer performance trends of RHA.

Application	Effect of RHA	Optimal Range	Key Mechanisms	References
SCM in Concrete	↑ Strength, ↓ Permeability	10–20%	Pozzolanic C-S-H formation, pore refinement	[42,79]
Chloride Resistance	↓ Ion Penetration	10–20%	Dense microstructure, reduced connectivity	[10,14]
Sulfate Resistance	↑ Significantly	10–30%	Consumption of $Ca(OH)_2$	[45,46,89]
Geopolymer Binder	↑ Compressive Strength	10–25%	Formation of N-A-S-H / C-A-S-H gels	[20]

9. Artificial intelligence and machine learning in RHA systems

The application of AI and ML has emerged as a powerful paradigm for modeling and optimizing properties of RHA-based composites and cementitious systems. These

data-driven techniques efficiently capture complex non-linear relationships between processing parameters, material composition, and performance, thereby accelerating materials design and reducing experimental overhead [43,44,79].

9.1. Prevalent AI/ML modeling approaches

Several ML algorithms have been successfully employed. Regression and response surface methodology quantify interaction effects of RHA content, particle size, and processing parameters on mechanical and tribological responses [37–39,124–127]. Artificial neural networks demonstrate high predictive accuracy ($R \approx 0.94–0.99$) for properties including tensile strength, wear rate, and concrete compressive strength [44]. Advanced algorithms, including SVR, random forest, and gradient boosting effectively model multivariable couplings and influence of hybrid reinforcements, often integrated with genetic algorithms or particle swarm optimization [43].

9.2. Predictive modeling for composite performance

For RHA-reinforced MMCs, ML models consistently identify dominant features such as RHA weight percentage, presence of hybrid reinforcements (SiC, CNTs), and fabrication route. Models predict minimum wear rate at 6–10 wt.% RHA, corroborating extensive experimental data [43]. Algorithms confirm optimal reinforcement range of 4–8 wt.% RHA for balancing hardness and tensile strength. For example, ANN models achieved prediction coefficients ($R \approx 0.95–0.99$) for tensile strength and wear rate. However, ML model accuracy depends heavily on quality and size of training datasets; generalizability across different RHA sources, combustion conditions, and impurity profiles remains a challenge requiring curated open-access databases.

9.3. Predictive modeling for cementitious and geopolymer systems

In concrete and geopolymer applications, ML models utilize mix design variables to predict performance. ANN and SVR models identify RHA fineness, replacement level, and curing age as most significant predictors of compressive strength [134]. ML accurately forecasts substantial reductions in chloride diffusion and water permeability at 10–20% cement replacement [42]. For geopolymers, models effectively capture non-linear effects of Na_2SiO_3/NaOH ratio, RHA content, and curing temperature on mechanical strength [41,59].

9.4. Model interpretation via explainable AI

Integration of explainable AI techniques such as SHAP provides critical insights into model decisions. SHAP analysis consistently identifies RHA content as most influential feature for strength, hardness, and permeability [128,129]. For tribological models, strong interaction effects between sliding velocity and applied load are revealed [43]. In concrete systems, fineness of RHA is paramount factor affecting pozzolanic activity and long-term durability [134].

Figure 9 illustrates the AI/ML workflow for RHA systems, including data acquisition, preprocessing, feature selection, model training, prediction, and experimental validation. The figure demonstrates that ML models can effectively

predict hardness, wear rate, tensile strength, compressive strength, and thermal properties based on processing and compositional variables. Comparative analysis also indicates that advanced ensemble and neural-network-based models generally exhibit higher prediction accuracy than conventional regression approaches. Adapted and modified from previous AI-assisted materials design studies [43,78].

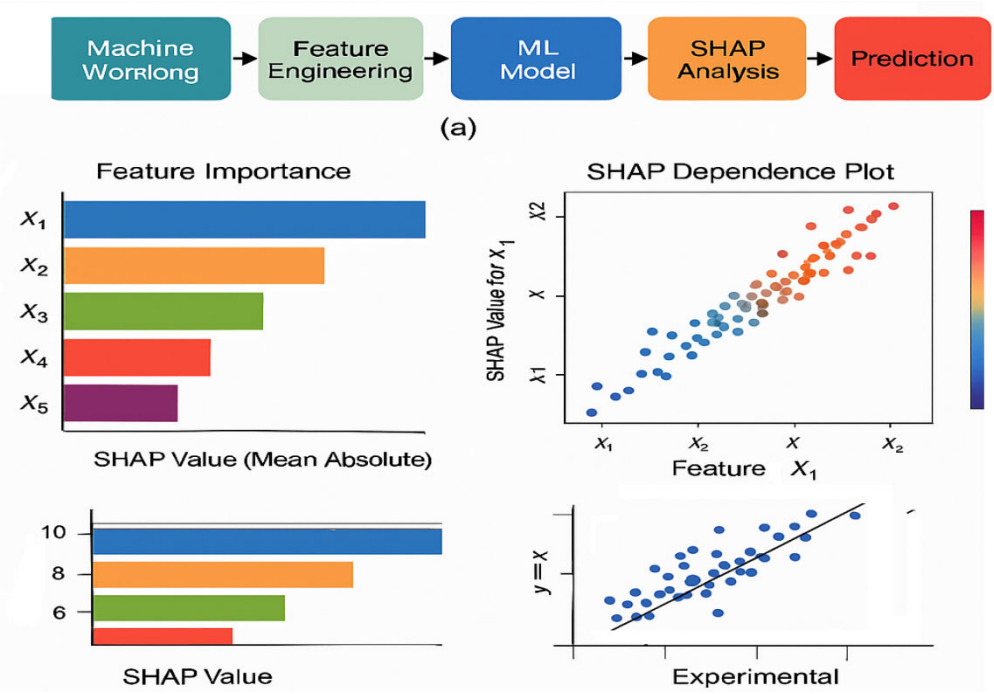

Figure 9. ML Workflow, Feature Importance, SHAP Dependency, Prediction vs. Experimental.

Table 9 reflects ML models applied to RHA-based materials, including ANN ($R \approx 0.94–0.99$ for strength/wear prediction), SVR (mechanical property optimization), random forest/gradient boosting (tribology and durability), and XAI-SHAP (feature importance). RHA content and fineness are consistently identified as the most influential features.

Table 9. ML Algorithms and Their Application Domains in RHA Studies.

ML Model	Application Domain	Key Influential Features	References
ANN	Strength, Wear, Compressive Strength	RHA wt.%, Sliding Velocity	[43,44,79]
SVR	Optimization of Mechanical Properties	RHA %, Hybrid Reinforcement	[43]
RF / Gradient Boosting	Tribology & Durability	Load, Velocity, RHA %, Fineness	[44,79]
RSM	Process & Response Optimization	Parameter Interaction Effects	[124,125]
XAI (SHAP)	Feature Importance & Sensitivity	RHA %, Fineness	[128,129]

10. Research roadmap and industrial scale-up

Despite significant progress, transition of RHA-based materials from laboratory to industry requires addressing key scientific and engineering challenges.

10.1. Foundational research priorities

Standardized RHA taxonomy should be developed and adopted (e.g., RHA-A95 for 95% amorphous silica, <45 μm) based on combustion conditions and purity, enabling reproducible research and specifications. Interface engineering database should systematically map effects of surface coatings (Si_3N_4, rare-earth oxides) and matrix alloys on interfacial shear strength and wettability. Mechanistic hybrid models must move beyond property reporting to develop micromechanical and multi-scale models predicting synergistic effects in RHA-SiC-CNT hybrid systems.

10.2. Process innovation for scale-up

Pilot-scale validation through open-access case studies for ≥100 kg batches of stir-cast RHA composites should quantify property variance and economic metrics (cost/kg, energy consumption). For instance, Udoye et al. (2021) [122] demonstrated stir-cast AA6061/RHA composites for cooling tower fan blades, achieving 32% hardness improvement at 6 wt.% RHA, indicating potential for non-structural automotive parts. Advanced low-cost routes such as friction stir processing of stir-cast blanks can locally enhance surface properties of low-cost bulk composites. AM feedstock development must solve powder flowability and melting consistency challenges to enable direct additive manufacturing of RHA-reinforced metal and geopolymer structures.

10.3. Data, AI, and sustainability integration

ML-ready datasets should curate open-access data linking RHA source, processing, fabrication, and full property profiles to fuel predictive AI models and enable inverse design. Explainable AI (XAI) for discovery should employ SHAP and sensitivity analysis not just for prediction but to uncover non-intuitive optimal parameter combinations (e.g., for geopolymer activation). Verified life-cycle assessment requires transparent, third-party verified LCA studies comparing RHA-MMCs to conventional composites (e.g., SiC/Al), quantifying net CO_2 savings across supply chain to justify green premiums.

10.4. Industrial and policy enablers

Supply chain development should foster partnerships between rice milling industries and material producers to ensure consistent, high-volume RHA supply with guaranteed specifications. Alignment with circular economy principles and ASTM/ACI standards for RHA as an SCM would accelerate acceptance in green construction markets. Codes and standards advocacy with standards organizations (ASTM, ACI) should develop provisional codes for RHA as SCM in concrete and as reinforcement in cast alloys. Demonstrator projects should support high-visibility applications (e.g., non-structural automotive parts, pervious concrete pavements) to build market confidence. **Table 10** prioritized research roadmap addressing scientific

and industrial barriers to RHA adoption. High-priority themes include RHA quality standardization, interface engineering, hybrid composite optimization, and AI/ML integration. Medium-priority themes focus on cementitious durability modeling and geopolymer activation science.

Table 10. Prioritized future research themes for RHA-based materials.

Theme	Priority	Rationale	References
RHA Quality Standardization	High	Ensures repeatability, enables industrial adoption	[33,62]
Interface Engineering	High	Improves bonding and mechanical reliability	[3,18,24]
Hybrid Composites Optimization	High	Enhances wear, toughness, multifunctionality	[21,130]
Cementitious Durability Modeling	Medium	Predict long-term behavior	[14,89,131]
Geopolymer Activation Science	Medium	Enables low-carbon binders	[20,132]
AI/ML Integration	High	Accelerates materials discovery	[43,45,46,133]

11. Conclusion

This review has presented a comprehensive processing-centric synthesis of four decades (1986–2025) of rice husk ash research, systematically linking combustion chemistry, purification, activation, and fabrication routes to microstructural evolution and final material performance across metal matrix composites, cementitious systems, and geopolymer binders. A consistent and universal outcome emerging from this analysis is the existence of an optimal reinforcement window of 4–10 wt.% RHA, within which significant improvements in hardness, tensile strength, wear resistance, dimensional stability, and durability are achieved, while avoiding deleterious effects of particle clustering and porosity observed at higher loadings.

The review further demonstrates that hybrid reinforcement strategies—notably RHA-SiC, RHA-B_4C, RHA-CNT, and RHA-graphite systems—offer a powerful pathway to overcome intrinsic brittleness of monolithic RHA composites. Through synergistic interface engineering and complementary functional mechanisms, these hybrid systems enable simultaneous enhancement of strength, wear resistance, fracture toughness, and tribological stability, thereby expanding the application envelope of RHA-based materials into demanding structural and functional domains.

Despite substantial progress documented, critical barriers to large-scale industrial deployment remain. Absence of standardized protocols for RHA characterization, including control of combustion conditions, impurity content, particle morphology, and surface chemistry, continues to limit reproducibility and cross-comparison of reported data. Moreover, although RHA is widely promoted as a sustainable material, reproducible and quantitative LCA data validating its CO_2 mitigation potential remain scarce, and pilot-scale validation of fabrication routes is still insufficient for reliable techno-economic translation.

12. Future outlook

Looking forward, transition of RHA from laboratory promise to industrial reality will depend on integration of data-driven material design frameworks. Convergence of experimental databases with AI/ML tools offers unprecedented opportunities for predictive optimization of composition-processing-property relationships, accelerated discovery of hybrid architectures, and inverse design of application-specific composites and binders. Establishing open, ML-ready datasets for RHA systems, combined with standardized testing methodologies and scalable manufacturing strategies, constitutes a central roadmap for future research.

Priority research directions include: (1) development of standardized RHA taxonomy and certification protocols; (2) systematic interface engineering databases for coating-matrix combinations; (3) pilot-scale demonstration projects with techno-economic validation; (4) third-party verified LCA studies to substantiate sustainability claims; and (5) integration of explainable AI for inverse materials design. Cross-sector partnerships between rice milling industries, material producers, and standards organizations will be essential to de-risk adoption.

In conclusion, rice husk ash represents a uniquely positioned, low-cost, and environmentally responsible resource for next-generation engineering materials. Through coordinated advances in processing control, hybrid composite design, standardization, sustainability validation, and AI-enabled optimization, RHA-based systems can play a transformative role in sustainable manufacturing and the emerging circular materials economy.

Author contributions: Conceptualization: AKM; Methodology: AKM; Investigation: AKM, TAA; Writing—Original Draft: AKM; Visualization: AKM, TAA; Validation: AKM, TAA; Project administration: AKM; Formal analysis: AKM, TAA; Data curation: AKM, TAA; Writing—Review & Editing: AKM, TAA; Resources: TAA

Acknowledgments: The authors sincerely thank the Department of Mechanical Engineering, SRM University, Delhi-NCR, Haryana, India, and the Department of Production & Industrial Engineering, BIT Mesra, Ranchi, India, for providing institutional support and research facilities. The authors also express gratitude to the researchers whose published works formed the foundation of this comprehensive review. No external funding was received for this study.

Availability of data: This review article is based entirely on published literature. No new primary data were generated or analyzed during this study. All data supporting the findings of this review are available from the cited references.

Nomenclature: AI—Artificial Intelligence, AM—Additive Manufacturing, AMC—Aluminum Matrix Composite, ANN—Artificial Neural Network, ASR—Alkali-Silica Reaction, ASTM—American Society for Testing and Materials, ACI—American Concrete Institute, B_4C—Boron Carbide, CNT—Carbon Nanotube, CTE—Coefficient of Thermal Expansion, C-S-H—Calcium-Silicate-Hydrate, EDM—Electrical Discharge Machining, EMI—Electromagnetic Interference, FGM—Functionally Graded Material, FSP—Friction Stir Processing, GA—Genetic Algorithm, GGBS—Ground Granulated Blast-Furnace Slag, GRA—Grey Relational

Analysis, HPC—High-Performance Concrete, HVOF—High-Velocity Oxy-Fuel, LCA—Life-Cycle Assessment, MIP—Mercury Intrusion Porosimetry, ML—Machine Learning, N-A-S-H—Sodium-Alumino-Silicate-Hydrate, PM—Powder Metallurgy, PSO—Particle Swarm Optimization, RF—Random Forest, RH—Rice Husk, RHA—Rice Husk Ash, RSM—Response Surface Methodology, SCC—Self-Compacting Concrete, SCM—Supplementary Cementitious Material, SEM—Scanning Electron Microscope, SHAP—SHapley Additive exPlanations, SiC—Silicon Carbide, Si_3N_4—Silicon Nitride, SPS—Spark Plasma Sintering, SVR—Support Vector Regression, XAI—Explainable Artificial Intelligence.

References

1. Abdulmalik SS, Ahmad R. Fabrication of AA6061-0/RHA Surface Composite via Friction Stir Processing. Applied Mechanics and Materials. 2014; 660: 214-218. doi: 10.4028/www.scientific.net/amm.660.214
2. Adediran AA, Alaneme KK, Oladele IO, Akinlabi ET. Wear characteristics of aluminium matrix composites reinforced with Si-based refractory compounds derived from rice husks. Stojanovic BCogent Engineering. 2020; 7(1). doi: 10.1080/23311916.2020.1826634
3. Adediran AA, Alaneme KK, Oladele IO, Akinlabi, ET. Microstructural characteristics and mechanical behaviour of aluminium matrix composites reinforced with Si-based refractory compounds derived from rice husk. Sánchez JCogent Engineering. 2021; 8(1). doi: 10.1080/23311916.2021.1897928
4. Ahamed AA, Ahmed R, Hossain MB, Billah M. Fabrication and Characterization of Aluminium-Rice Husk Ash Composite Prepared by Stir Casting Method. Rajshahi University Journal of Science and Engineering. 2016; 44: 9-18. doi: 10.3329/rujse.v44i0.30361
5. Udoye NE, Nnamba OJ, Fayomi OSI, et al. Corrosion Performance of AA6061/Rice Husk Ash Composite for Engineering Application. IOP Conference Series: Materials Science and Engineering. 2021; 1107(1): 12121. doi: 10.1088/1757-899x/1107/1/0121211.
6. Aigbodion VS, Ozor PO, Eke MN, Nwoji CU. Explicit microstructure, corrosion, and stress analysis of value-added Al-3.7%Cu-1.4%Mg/1.5% rice husk ash nanoparticles for pump impeller application. Chemical Data Collections. 2021; 33: 100675. doi: 10.1016/j.cdc.2021.100675
7. Alaneme KK, Adewale TM. Influence of rice husk ash-silicon carbide weight ratios on the mechanical behaviour of Al-Mg-Si alloy matrix hybrid composites. Tribology in Industry. 2013; 35(2): 163. doi: 10.1016/j.jmrt.2013.03.012
8. Alaneme KK, Akintunde IB, Olubambi PA, Adewale TM. Fabrication characteristics and mechanical behaviour of rice husk ash–Alumina reinforced Al-Mg-Si alloy matrix hybrid composites. Journal of Materials Research and Technology. 2013; 2(1): 60-67. doi: 10.1016/j.jmrt.2013.03.012
9. Alaneme KK, Olubambi PA. Corrosion and wear behaviour of rice husk ash—Alumina reinforced Al–Mg–Si alloy matrix hybrid composites. Journal of Materials Research and Technology. 2013; 2(2): 188-194. doi: 10.1016/j.jmrt.2013.02.005
10. Alaneme KK, Sanusi KO. Microstructural characteristics, mechanical and wear behaviour of aluminium matrix hybrid composites reinforced with alumina, rice husk ash and graphite. Engineering Science and Technology, an International Journal. 2015; 18(3): 416-422. doi: 10.1016/j.jestch.2015.02.003
11. Alaneme KK, Anabaranze YO, Oke SR. Softening resistance, dimensional stability and corrosion behaviour of alumina and rice husk ash reinforced aluminium matrix composites subjected to thermal cycling. Tribology in Industry, 2015; 37(2): 204.
12. Alaneme KK, Ajayi OJ. Microstructure and mechanical behaviour of Al-Mg-Si alloy matrix hybrid composites reinforced with rice husk ash and silicon carbide. Journal of King Saud University - Engineering Sciences. 2017; 29(2): 172-177. doi: 10.1016/j.jksues.2015.06.004
13. Alaneme KK, Bodunrin MO, Awe AA. Microstructure, mechanical and fracture properties of groundnut shell ash and silicon carbide dispersion strengthened aluminium matrix composites. Journal of King Saud University - Engineering Sciences. 2018; 30(1): 96-103. doi: 10.1016/j.jksues.2016.01.001
14. Ali I, Motgi P. A study on mechanical properties of concrete incorporating rice husk ash as partial replacement of cement. Materials Today: Proceedings, 2021; 47: 5525-5530.

15. Alweendo ST, Shongwe MB, Olubambi PA, Potgieter JH. Spark plasma sintering of Al-SiC metal matrix composites: a review. Journal of Materials Research and Technology, 2020; 9(5): 10129-10147.
16. Andrade-Tacca CA, Andrade-Tacca MC, Rojas R. Use of rice husk ash in the production of sustainable concrete. Revista de la Construcción, 2019; 18(2): 245-256.
17. Arora S, Sharma S. Influence of rice husk ash on mechanical properties of aluminium matrix composites: a review. Materials Today: Proceedings, 2020; 21: 1450-1455.
18. Arora S, Sharma S. Mechanical and tribological properties of rice husk ash reinforced Al-4.5%Cu alloy composites processed by spark plasma sintering. Silicon, 2021; 13(8): 2675-2688.
19. Awad AY, Moosa A, Al-Mosawi, AI. Effect of rice husk ash addition on mechanical properties of aluminium matrix composite. International Journal of Mechanical Engineering and Technology, 2018; 9(6): 456-463.
20. Bahrami A, Pech-Canul MI, Soltani N. Fabrication and properties of Al/SiC/RHA hybrid composites by pressureless infiltration. Materials Science Forum, 2015; 828-829: 367-372.
21. Bahrami A, Pech-Canul MI, Gutiérrez CA, Soltani N. Microstructure and properties of bilayer-graded Al-matrix composites by one-step pressureless infiltration of B4C/rice-husk ash preforms. MRS Online Proceedings Library, 2016; 1820: imrc2015s6d-0011. https://doi.org/10.1557/opl.2016.68
22. Bahrami A, Pech-Canul MI, Soltani N, et al. Tailoring microstructure and properties of bilayer-graded Al/B4C/MgAl2O4 composites by single-stage pressureless infiltration. Journal of Alloys and Compounds. 2017; 694: 408-418. doi: 10.1016/j.jallcom.2016.09.284
23. Bahrami A, Soltani N, Soltani S, et al. Mechanical, thermal and electrical properties of monolayer and bilayer graded Al/SiC/rice husk ash (RHA) composite. Journal of Alloys and Compounds. 2017; 699: 308-322. doi: 10.1016/j.jallcom.2016.12.339
24. Bahrami A, Soltani N, Pech-Canul MI, et al. Bilayer graded Al/B 4 C/rice husk ash composite: Wettability behavior, thermo-mechanical, and electrical properties. Journal of Composite Materials. 2018; 52(27): 3745-3758. doi: 10.1177/0021998318769993
25. Parveez B, Maleque MA, Jamal NA. Influence of agro-based reinforcements on the properties of aluminum matrix composites: a systematic review. Journal of Materials Science. 2021; 56(29): 16195-16222. doi: 10.1007/s10853-021-06305-2
26. Singari RM, Mathiyazhagan K, Kumar H, et al. Advances in Manufacturing and Industrial Engineering: Select Proceedings of ICAPIE 2019. Springer Nature Singapore; 2021. doi: 10.1007/978-981-15-8542-5
27. Yadav AK, Pandey KM, Dey A. Aluminium Metal Matrix Composite with Rice Husk as Reinforcement: A Review. Materials Today: Proceedings. 2018; 5(9): 20130-20137. doi: 10.1016/j.matpr.2018.06.381
28. Chandrasekhar S, Satyanarayana KG, Pramada PN, Raghavan P, Gupta TN. Review processing, properties and applications of reactive silica from rice husk-an overview. Journal of Materials Science, 2003; 38(15): 3159-3168. https://doi.org/10.1023/A:1025157114800
29. Della VP, Kühn I, Hotza D. Rice husk ash as an alternate source for active silica production. Materials Letters, 2002; 57(4): 818-821. https://doi.org/10.1016/S0167-577X(02)00879-0
30. Real C, Alcalá MD, Criado JM. Preparation of Silica from Rice Husks. Journal of the American Ceramic Society. 1996; 79(8): 2012-2016. doi: 10.1111/j.1151-2916.1996.tb08931.x
31. Soltani N, Bahrami A, Pech-Canul MI, et al. Review on the physicochemical treatments of rice husk for production of advanced materials. Chemical Engineering Journal. 2015; 264: 899-935. doi: 10.1016/j.cej.2014.11.056
32. Jyothi PN, Kumar B. Comparison of mechanical properties of Al-5% Si alloy reinforced with cow dung ash and rice husk ash. International Journal of Latest Research in Engineering and Technology, 2015; 1: 55-58.
33. Holzschuh GG, Dörr DS, Moraes JAR, et al. Metal matrix production: Casting of recycled aluminum cans and incorporation of rice husk ash and magnesium. Journal of Composite Materials. 2020; 54(22): 3229-3241. doi: 10.1177/0021998320911964
34. Das S, Dan TK, Prasad SV, et al. Aluminium alloy—rice husk ash particle composites. Journal of Materials Science Letters. 1986; 5(5): 562-564. doi: 10.1007/bf01728691
35. Dora SP, Chintada S, Palukuri TR, et al. Energy dissipation in WC-Co coated A356.2/RHA composites. Engineering Science and Technology, an International Journal. 2020; 23(5): 1285-1290. doi: 10.1016/j.jestch.2020.04.001

36. Escalera-Lozano R, Gutiérrez CA, Pech-Canul MA, et al. Degradation of Al/SiCp composites produced with rice-hull ash and aluminum cans. Waste Management. 2008; 28(2): 389-395. doi: 10.1016/j.wasman.2006.12.005
37. Durowoju MO, Agunsoye JO, Mudashiru LO, et al. Optimization of Stir Casting Process Parameters to Improve the Hardness Property of Al/RHA Matrix Composites. European Journal of Engineering and Technology Research. 2017; 2(11): 5-12. doi: 10.24018/ejeng.2017.2.11.498
38. Muni RN, Singh J, Kumar V, Sharma S. Parametric optimization of rice husk ash, copper, magnesium reinforced aluminium matrix hybrid composite processed by EDM. ARPN Journal of Engineering and Applied Sciences, 2019; 14: 3832-3839.
39. Muni RN, Singh J, Kumar V, Sharma S. Influence of rice husk ash, Cu, Mg on the mechanical behaviour of Aluminium Matrix hybrid composites. International Journal of Applied Engineering Research, 2019; 14(8): 28-34.
40. Guo Z, Chen Z, Yang X, et al. The Influence of Rice Husk Ash Incorporation on the Properties of Cement-Based Materials. Materials. 2025; 18(2): 460. doi: 10.3390/ma18020460
41. Hamada HM, Al-Attar A, Beddu S, et al. Impact of rice husk ash on geopolymer concrete: A literature review and future directions. Case Studies in Construction Materials. 2025; 22: e04476. doi: 10.1016/j.cscm.2025.e04476
42. Jing Y, Lee JC, Moon WC, Ng JL, Yew MK, Jin Y. Durability and environmental evaluation of rice husk ash sustainable concrete containing carbon nanotubes. Scientific Reports, 2025; 15(1), 4352. https://doi.org/10.1038/s41598-025-88927-z
43. Mishra AK. Machine learning-based prediction of coefficient of friction and specific wear rate in aluminum-based metal matrix composites. Tribology - Materials, Surfaces & Interfaces. 2025; 20(1): 31-42. doi: 10.1177/17515831251401637
44. Saravanan SD, Senthilkumar M. Prediction of tribological behaviour of rice husk ash reinforced aluminum alloy matrix composites using artificial neural network. Russian Journal of Non-Ferrous Metals. 2015; 56(1): 97-106. doi: 10.3103/s1067821215010174
45. Vinod B, Ramanathan S, Anandajothi M. Effect of Organic and Inorganic Reinforcement on Tribological Behaviour of Aluminium A356 Matrix Hybrid Composite. Journal of Bio- and Tribo-Corrosion. 2018; 4(3). doi: 10.1007/s40735-018-0157-9
46. Vinod B, Ramanathan S, Ananthi V, et al. Fabrication and Characterization of Organic and In-Organic Reinforced A356 Aluminium Matrix Hybrid Composite by Improved Double-Stir Casting. Silicon. 2018; 11(2): 817-829. doi: 10.1007/s12633-018-9881-5
47. Krishnarao RV, Subrahmanyam J, Jagadishkumar T. Preparation of Black Amorphous Silica from Rice Husks. Transactions of the Indian Ceramic Society. 2001; 60(2): 95-99. doi: 10.1080/0371750x.2001.10799976
48. Mohd Joharudin NF, Abdul Latif N, Mustapa MS, et al. Effect of Burning Temperature on Rice Husk Silica as Reinforcement of Recycled Aluminium Chip AA7075. Journal of Advanced Research in Fluid Mechanics and Thermal Sciences. 2020; 68(1): 125-132. doi: 10.37934/arfmts.68.1.125132
49. Joharudin NFM, Latif NA, Mustapa MS, Badarulzaman NA. Effects of untreated and treated rice husk ash (RHA) on physical properties of recycled aluminium chip AA7075. International Journal of Integrated Engineering, 2020; 12(1): 132-137.
50. Lee JH, Kwon JH, Lee J-W, et al. Preparation of high purity silica originated from rice husks by chemically removing metallic impurities. Journal of Industrial and Engineering Chemistry. 2017; 50: 79-85. doi: 10.1016/j.jiec.2017.01.033
51. Sun L, Gong K. Silicon-Based Materials from Rice Husks and Their Applications. Industrial & Engineering Chemistry Research. 2001; 40(25): 5861-5877. doi: 10.1021/ie010284b
52. Singh RP. Synthesis and characterisation of Al-Mg-SiO2 particulate composite prepared by nanostructured silica from rice husk ash. Materials Today: Proceedings. 2021; 37: 3148-3153. doi: 10.1016/j.matpr.2020.09.043
53. Prasad DS, Krishna AR. Production and mechanical properties of A356.2/RHA composites. International Journal of Advanced Science and Technology, 2011; 33: 51-58.
54. Pradhan MK, Tiwari S. Investigation of mechanical properties and electrical discharge machining of LM25-RHA metal matrix composite. International Journal of Machining and Machinability of Materials. 2017; 19(5): 457. doi: 10.1504/ijmmm.2017.087619
55. Soltani N, Bahrami A, Pech-Canul MI, et al. Surface modification of rice-husk ash (RHA) by Si3N4 coating to promote its wetting by Al-Mg-Si alloys. Materials Chemistry and Physics. 2018; 203: 223-234. doi: 10.1016/j.matchemphys.2017.10.009

56. Soltani N, Bahrami A, Pech-Canul MI, et al. Improving the Interfacial Reaction Between Cristobalite Silica from Rice Husk and Al–Mg–Si by CVD-Si3N4 Deposition. Waste and Biomass Valorization. 2019; 11(7): 3789-3799. doi: 10.1007/s12649-019-00706-w
57. Moosa A, Awad AY. Effect of rare earth addition on wear properties of aluminum alloy-rice husk ash/yttrium oxide hybrid composites. International Journal of Current Engineering and Technology, 2016; 6(3): 788-798.
58. Moosa A, Awad AY. Influence of rice husk ash-yttrium oxide addition on the mechanical properties behavior of aluminum alloy matrix hybrid composites. International Journal of Current Engineering and Technology, 2016; 6(3): 804-812.
59. Onsongo SK, Olukuru J, Munyao OM, et al. The role of agricultural ashes (rice husk ash, coffee husk ash, sugarcane bagasse ash, palm oil fuel ash) in cement production for sustainable development in Africa. Discover Sustainability. 2025; 6(1). doi: 10.1007/s43621-025-00841-6
60. Chinnamahammad Bhasha A, Balamurugan K. Fabrication and property evaluation of Al 6061 + x% (RHA + TiC) hybrid metal matrix composite. SN Applied Sciences. 2019; 1(9). doi: 10.1007/s42452-019-1016-0
61. Haque MH, Ahmed R, Khan M, Shahriar S. Fabrication, reinforcement and characterization of metal matrix composites (MMCs) using rice husk ash and aluminium alloy (A-356.2). International Journal of Scientific and Engineering Research, 2016; 7(3): 28-35.
62. Hossain MdR, Ali MdH, Amin MdA, et al. Fabrication and Performance Test of Aluminium Alloy-Rice Husk Ash Hybrid Metal Matrix Composite as Industrial and Construction Material. International Journal of Engineering Materials and Manufacture. 2017; 2(4): 94-102. doi: 10.26776/ijemm.02.04.2017.03
63. P. NANDA K, P.S.RAVI K, G. RANGA J, . Fabrication and Characteristics of AMC/RHA Functionally Graded Materials by Controlled Mold Filling. i-manager's Journal on Material Science. 2016; 4(3): 12. doi: 10.26634/jms.4.3.8242
64. Sathiesh Kumar N. Fabrication and characterization of Al7075 / RHA /Mica composite by squeeze casting. Materials Today: Proceedings. 2021; 37: 750-753. doi: 10.1016/j.matpr.2020.05.769
65. Mohd Joharudin NF, Abdul Latif N, Mustapa MS, et al. Effect of amorphous silica by rice husk ash on physical properties and microstructures of recycled aluminium chip AA7075. Materialwissenschaft und Werkstofftechnik. 2019; 50(3): 283-288. doi: 10.1002/mawe.201800229
66. Deshmukh PY, Peshwe DR, Bhatt J, et al. Synthesis and Characterization of Al–Mg–SiO2 Particulate Composite Using Amorphous SiO2 from Rice Husk Ash. Transactions of the Indian Institute of Metals. 2011; 64(6): 575-581. doi: 10.1007/s12666-011-0083-8
67. Dwivedi SP, Sharma P, Saxena A. Utilization of waste spent alumina catalyst and agro-waste rice husk ash as reinforcement materials with scrap aluminium alloy wheel matrix. Proceedings of the Institution of Mechanical Engineers, Part E: Journal of Process Mechanical Engineering. 2020; 234(6): 543-552. doi: 10.1177/0954408920930634
68. Deshmukh P, Pathak S. Influence of Varying SiO2 % on the Mechanical Properties of Al Based MMC. Transactions of the Indian Institute of Metals. 2012; 65(6): 741-745. doi: 10.1007/s12666-012-0196-8
69. Shaikh MBN, Arif S, Aziz T, et al. Microstructural, mechanical and tribological behaviour of powder metallurgy processed SiC and RHA reinforced Al-based composites. Surfaces and Interfaces. 2019; 15: 166-179. doi: 10.1016/j.surfin.2019.03.002
70. Siddharth D, Mahato N, Rao JB. Synthesis & characterization of RHA (Rice Husk Ash) particulates reinforced A7075 composites. Journal of Manufacturing Engineering, 2017; 12(2): 55-61.
71. Gladston JAK, Sheriff NM, Dinaharan I, Selvam JDR. Production and characterization of rich husk ash particulate reinforced AA6061 aluminum alloy composites by compocasting. Transactions of Nonferrous Metals Society of China, 2015; 25(3): 683-691. https://doi.org/10.1016/S1003-6326(15)63653-6
72. Gladston JAK, Dinaharan I, Sheriff NM, et al. Dry sliding wear behavior of AA6061 aluminum alloy composites reinforced rice husk ash particulates produced using compocasting. Journal of Asian Ceramic Societies. 2017; 5(2): 127-135. doi: 10.1016/j.jascer.2017.03.005
73. Subrahmanyam APSVR, Naresh G, Venkatesu V. Microstructure and mechanical properties of rice husk ash reinforced aluminium alloy (A356.2) metal matrix composite. IOSR Journal of Engineering, 2018; 8: 36-42.
74. Dinaharan I, Kalaiselvan K, Murugan N. Influence of rice husk ash particles on microstructure and tensile behavior of AA6061 aluminum matrix composites produced using friction stir processing. Composites Communications. 2017; 3: 42-46. doi: 10.1016/j.coco.2017.02.001

75. Maji P, Ghosh SK, Nath RK, et al. Microstructural, mechanical and wear characteristics of aluminum matrix composites fabricated by friction stir processing. Journal of the Brazilian Society of Mechanical Sciences and Engineering. 2020; 42(4). doi: 10.1007/s40430-020-02279-5
76. Marini CD, Fatchurrohman N. Microstructure and hardness performance of AA6061 aluminium composite using friction stir processing. IOP Conference Series: Materials Science and Engineering. 2018; 342: 12077. doi: 10.1088/1757-899x/342/1/012077
77. Patil NA, Safwan A, Pedapati SR. Effect of deposition methods on microstructure and mechanical properties of Al 7075 alloy-rice husk ash surface composites using friction stir processing. Materials Today: Proceedings. 2020; 29: 143-148. doi: 10.1016/j.matpr.2020.05.639
78. Seetharaman S, Subramanian J, Singh RA, et al. Mechanical Properties of Sustainable Metal Matrix Composites: A Review on the Role of Green Reinforcements and Processing Methods. Technologies. 2022; 10(1): 32. doi: 10.3390/technologies10010032
79. Kashem A, Karim R, Das P, et al. Compressive strength prediction of sustainable concrete incorporating rice husk ash (RHA) using hybrid machine learning algorithms and parametric analyses. Case Studies in Construction Materials. 2024; 20: e03030. doi: 10.1016/j.cscm.2024.e03030
80. Shoba C, Ramanaiah N, Rao DN. Optimizing The Machining Parameters For Minimum Surface Roughness In Turning Al/6% SiC/6%RHA Hybrid Composites. Procedia Materials Science. 2015; 10: 220-229. doi: 10.1016/j.mspro.2015.06.044
81. Sathiparan N, Subramaniam DN. Optimizing fly ash and rice husk ash as cement replacements on the mechanical characteristics of pervious concrete. Sustainable Structures, 2025; 5(1): 100045. https://doi.org/10.1016/j.susstr.2025.100045
82. Siva Prasad D, Shoba C. Hybrid composites–a better choice for high wear resistant materials. Journal of Materials Research and Technology. 2014; 3(2): 172-178. doi: 10.1016/j.jmrt.2014.03.004
83. Subrahmanyam APSVR, Madhukiran J, Naresh G, et al. Fabrication and Characterization of Al356.2, Rice Husk Ash and Fly Ash Reinforced Hybrid Metal Matrix Composite. International Journal of Advanced Science and Technology. 2016; 94: 49-56. doi: 10.14257/ijast.2016.94.05
84. Narasaraju G, Raju DL. Characterization of Hybrid Rice Husk and Fly ash-Reinforced Aluminium alloy (AlSi10Mg) Composites. Materials Today: Proceedings. 2015; 2(4-5): 3056-3064. doi: 10.1016/j.matpr.2015.07.245
85. Shoba C, Ramanaiah N, Rao DN. Influence of dislocation density on the residual stresses induced while machining Al/SiC/RHA hybrid composites. Journal of Materials Research and Technology. 2015; 4(3): 273-277. doi: 10.1016/j.jmrt.2014.12.010
86. Khan T, Wahab SABA, Chaudhuri M. Arsenic(III) immobilization on rice husk silica. 2011 National Postgraduate Conference. 2011: 1-4. doi: 10.1109/natpc.2011.6136347
87. Dwivedi SP, Srivastava A, Kumar A, Nandan B. Microstructure and mechanical behaviour of RHA and B4C reinforced aluminium alloy hybrid metal matrix composite. Indian Journal of Engineering & Materials Sciences, 2017; 24: 133-140.
88. Saravanan SD, Senthilkumar M. Mechanical behavior of aluminum (AlSi10Mg)-RHA composite. International Journal of Engineering and Technology, 2014; 5(6): 4834-4840.
89. Vasamsetti S, Dumpala L, Subbarao VV. Synthesis, characterization and hardness studies of nano rice husk ash reinforced Al6061 nanocomposites. Journal of Engineering Science and Technology, 2018; 13(9): 2916-2929.
90. D. Manoj Kumar et al., DMKeal, . Synthesis Characterization and Mechanical Behavior of Rice Husk Ash Reinforced Al-20mg 10 Cu Alloy Matrix Hybrid Composites. International Journal of Mechanical and Production Engineering Research and Development. 2018; 8(1): 111-118. doi: 10.24247/ijmperdfeb201813
91. Mishra P, Mishra P, Rana RS. Effect of Rice Husk ash Reinforcements on Mechanical properties of Aluminium alloy (LM6) Matrix Composites. Materials Today: Proceedings. 2018; 5(2): 6018-6022. doi: 10.1016/j.matpr.2017.12.205
92. Udoye NE, Fayomi OSI, Inegbenebor AO. Fractography and Tensile Properties of AA6061 Aluminium Alloy/Rice Husk Ash Silicon Nanocomposite. International Journal of Chemical Engineering. 2020; 2020: 1-8. doi: 10.1155/2020/8818224
93. Saravanan SD, Kumar MS. Effect of Mechanical Properties on Rice Husk Ash Reinforced Aluminum Alloy (AlSi10Mg) Matrix Composites. Procedia Engineering. 2013; 64: 1505-1513. doi: 10.1016/j.proeng.2013.09.232
94. Subrahmanyam APSVR, Narsaraju G, Rao BS. Effect of Rice Husk ash and Fly ash Reinforcements on Microstructure and Mechanical properties of Aluminium alloy (AlSi10Mg) Matrix Composites. International Journal of Advanced Science and Technology. 2015; 76: 1-8. doi: 10.14257/ijast.2015.76.01

95. Prasad DS, Krishna AR. Tribological properties of A356.2/RHA composites. Journal of Materials Science & Technology, 2012; 28(4): 367-372. https://doi.org/10.1016/S1005-0302(12)60069-3
96. Siva Prasad D, Shoba C. Experimental evaluation onto the damping behavior of Al/SiC/RHA hybrid composites. Journal of Materials Research and Technology. 2016; 5(2): 123-130. doi: 10.1016/j.jmrt.2015.08.001
97. Muralimohan R, Kempaiah UN, Seenappa. Influence of rice husk ash and B4C on mechanical properties of ADC 12 alloy hybrid composites. Materials Today: Proceedings. 2018; 5(11): 25562-25569. doi: 10.1016/j.matpr.2018.10.363
98. Ragupathi P, Kumar NS. Optimization of machining parameters for minimal temperature in cylindrical grinding of Al7075/RHA composite. Materials Today: Proceedings. 2021; 37: 745-749. doi: 10.1016/j.matpr.2020.05.760
99. Thiagarajan G, Abdul Latif N, Mohd Joharudin NF. Preliminary Study on Crystallinity of Rice Husk Ash Reinforcement for Metal Matrix Composite. Advanced Research in Natural Fibers, 2020; 2(1): 21-24.
100. Soltani N, Soltani S, Bahrami A, et al. Electrical and thermomechanical properties of CVI- Si3N4 porous rice husk ash infiltrated by Al-Mg-Si alloys. Journal of Alloys and Compounds. 2017; 696: 856-868. doi: 10.1016/j.jallcom.2016.12.051
101. Pattnayak A, Madhu N, Panda AS, et al. A Comparative study on mechanical properties of Al-SiO2 composites fabricated using rice husk silica in crystalline and amorphous form as reinforcement. Materials Today: Proceedings. 2018; 5(2): 8184-8192. doi: 10.1016/j.matpr.2017.11.507
102. Udoye NE, Inegbenebor AO, Fayomi OSI. Corrosion Performance and Wear Behaviour of AA6061 Reinforced Hybrid: Nano-Rice Husk Ash/Clay Particulate for Cooling Tower Fan Blade in 0.75 M H2SO4. Journal of Bio- and Tribo-Corrosion. 2020; 6(2). doi: 10.1007/s40735-020-00359-6
103. Ghosh S, Basak R, Rao AS. Study of Mechanical and Tribological Characteristics of Aluminium Alloy Reinforced with Rice Husk Ash. International Journal of Engineering Research & Technology, 2018; 7(6): 1-6
104. Senthilkumar M, Saravanan S, Shankar S. Dry sliding wear and friction behavior of aluminum–rice husk ash composite using Taguchi's technique. Journal of Composite Materials. 2014; 49(18): 2241-2250. doi: 10.1177/0021998314545185
105. S SP, Sudhakaran R. Tribological Behavoiur of Silicon Carbide/ Rice Husk ash Reinforced Al7075 Hybrid Composites Using Optimization Techniques. International Journal of Engineering Research & Technology. 2021; 10(4): 1-8. doi: 10.21203/rs.3.rs-621659/v1
106. Saravanan SD, Senthilkumar M, Shankar S. Effect of Particle Size on Tribological Behavior of Rice Husk Ash–Reinforced Aluminum Alloy (AlSi10Mg) Matrix Composites. Tribology Transactions. 2013; 56(6): 1156-1167. doi: 10.1080/10402004.2013.831962
107. Verma N, Vettivel SC. Characterization and experimental analysis of boron carbide and rice husk ash reinforced AA7075 aluminium alloy hybrid composite. Journal of Alloys and Compounds. 2018; 741: 981-998. doi: 10.1016/j.jallcom.2018.01.185
108. Dwivedi SP, Mishra VR. Physico-Chemical, Mechanical and Thermal Behaviour of Agro-waste RHA-Reinforced Green Emerging Composite Material. Arabian Journal for Science and Engineering. 2019; 44(9): 8129-8142. doi: 10.1007/s13369-019-03784-z
109. Gaikwad SP, Kale PT, Gadhave SL. Corrosion and Wear Characteristics of A356.0-SiC-RHA Hybrid Composite. International Journal of Engineering Research and Technology, 2018; 7(4): 1-6.
110. Idusuyi N, Oviroh PO, Adekoya AH. A Study on the Corrosion and Mechanical Properties of an Al6063 Reinforced With Egg Shell Ash and Rice Husk Ash. In: ASME International Mechanical Engineering Congress and Exposition. 2018:52170.
111. Joseph OO, Dirisu JO, Atiba J, et al. Mechanical, and corrosive properties of AA7075 aluminium reinforced with rice husk ash particulates. Materials Research Express. 2023; 10(11): 116520. doi: 10.1088/2053-1591/ad0dd3
112. Nithyanandhan T, Sivaraman P, Ramamoorthi R, et al. Enhancement of corrosion behaviour of AL6061- B4C-RHA reinforced hybrid composite. Materials Today: Proceedings. 2020; 33: 372-377. doi: 10.1016/j.matpr.2020.04.167
113. Gaikwad SP. Comparison of Damping Characteristics of Aluminium A356.0 with Respect to Al-SiC-RHA Hybrid Composite. International Journal of Engineering Research, 2017; 7(5): 1-5.
114. Taniş NA, Okur O, Duran O, et al. An Investigation of Production and Properties of RHA Reinforced Hybrid Composites by Vacuum Infiltration Method. International Journal of Engineering Research and Development. 2021; 13(2): 704-710. doi: 10.29137/umagd.913816
115. Prasad DS, Shoba C, Ramanaiah N. Investigations on mechanical properties of aluminum hybrid composites. Journal of Materials Research and Technology. 2014; 3(1): 79-85. doi: 10.1016/j.jmrt.2013.11.002

116. Moulssewaran SK, Gopal E, Ramesh KPM, Ravikumar M, Sakthivel R. Structural And Thermal Study Of Aluminum Hybrid Composite Alloy Reinforced With Silicon Carbide And Rice Husk Ash For Automobile Brake Drum. Annals of the Faculty of Engineering Hunedoara, 2017; 15(4): 31-39.
117. Najib MAM, Ariff AHM, Tahir SM, et al. Microstructural, physical and mechanical analysis of rha pore modified porous alumina with aluminum as reinforcement. ASEAN Engineering Journal. 2019; 9(1): 29-43. doi: 10.11113/aej.v9.15506
118. Olorunyolemi OC, Ogunsanya OA, Akinwande AA, et al. Influence of SiO2 form the rice husk ash and coal fly ash particles on the mechanical behaviour and grain characteristics of the stir-casted hybrid composites. Materials Today: Proceedings. 2022; 62: 1234-1242. doi: 10.21203/rs.3.rs-1269445/v1
119. Tanis NA, Oku O, Duran O, Dele-Afolabi TT, Hanim MA, Calin R. An Investigation on the Properties of RHA and Al2O3 Reinforced Hybrid Composites. International Journal of Engineering Research and Development, 2019: 57-63.
120. Verma N, Vettivel SC, Rao P, et al. Processing, tool wear measurement using machine vision system and optimization of machining parameters of boron carbide and rice husk ash reinforced AA 7075 hybrid composite. Materials Research Express. 2019; 6(8): 0865f3. doi: 10.1088/2053-1591/ab25091.
121. Singh CV, Pachauri P, Dwivedi SP, et al. Formation of functionally graded hybrid composite materials with Al2O3 and RHA reinforcements using friction stir process. Australian Journal of Mechanical Engineering. 2019; 20(1): 141-154. doi: 10.1080/14484846.2019.1679583
122. Udoye NE, Nnamba OJ, Fayomi OSI, et al. Analysis on mechanical properties of AA6061/Rice husk ash composites produced through stir casting technique. Materials Today: Proceedings. 2021; 43: 1415-1420. doi: 10.1016/j.matpr.2020.09.178
123. Gupta V, Singh B, Mishra R. Tribological characteristics of AA7075 composites reinforced with rice husk ash and carbonized eggshells. Proceedings of the Institution of Mechanical Engineers, Part L: Journal of Materials: Design and Applications. 2021; 235(11): 2600-2613. doi: 10.1177/14644207211025810
124. Dwivedi SP, Dwivedi G. Utilization of RHA in development of hybrid composite by electromagnetic stir casting technique using RSM. Journal of Metals, Materials and Minerals. 2019; 29(4). doi: 10.55713/jmmm.v29i4.538
125. Dwivedi SP, Dwivedi G. Utilization of RHA in development of green composite material using RSM. Journal of the Mechanical Behavior of Materials. 2019; 28(1): 20-28. doi: 10.1515/jmbm-2019-0004
126. Kumar A, Kumar M. Mechanical and dry sliding wear behaviour of B4C and rice husk ash reinfroced Al 7075 alloy hybrid composite for armors application by using taguchi techniques. Materials Today: Proceedings. 2020; 27: 2617-2625. doi: 10.1016/j.matpr.2019.11.075
127. Saravanan SD, Kumar SS. Optimization of Casting Parameters on Al/RHA Composite Using Taguchi Method. Advanced Materials Research. 2014; 984-985: 291-296. doi: 10.4028/www.scientific.net/amr.984-985.291
128. Alyami, M., Alqahtani, A., Khan, M.A. and Ullah, S. Explainable machine learning for predicting compressive strength of rice husk ash concrete. Case Studies in Construction Materials, 2024; 20, p.e03125. https://doi.org/10.1016/j.cscm.2024.e03125
129. Amin MN, Khan K, Abu-Arab AM, Al-Hasani A. Prediction of compressive strength of rice husk ash concrete using SHAP analysis and machine learning. Materials, 2023; 16(8): 3124
130. Kumar AP, Naik BJ, Rao CV, Rao SR. Optimization of casting parameters for casting of AL/RHA/RM hybrid composites using Taguchi method. International Journal of Engineering Trends and Technology, 2013; 4(8): 3284-3288.
131. Rattanasak U, Chindaprasirt P, Suwanvitaya P. Development of high volume rice husk ash alumino silicate composites. International Journal of Minerals, Metallurgy, and Materials. 2010; 17(5): 654-659. doi: 10.1007/s12613-010-0370-0
132. Uddin MN, Li L-Z, Deng B-Y, et al. Interpretable XGBoost–SHAP machine learning technique to predict the compressive strength of environment-friendly rice husk ash concrete. Innovative Infrastructure Solutions. 2023; 8(5). doi: 10.1007/s41062-023-01122-9
133. Virkunwar AK, Ghosh S, Basak R. Wear characteristics optimization of Al6061-Rice husk ash metal matrix composite using Taguchi method. Materials Today: Proceedings. 2019; 19: 546-550. doi: 10.1016/j.matpr.2019.07.731
134. Yang YP, Deng YG, Chen LS. Properties of high-volume rice husk ash UHPC with various fineness. Construction and Building Materials, 2025; 458: 139614. https://doi.org/10.1016/j.conbuildmat.2025.139614